Recent progress in the field of electron correlation

G. Senatore

Dipartimento di Fisica Teorica, Università di Trieste, I-34014 Grignano (TS), Italy

N. H. March

Department of Theoretical Chemistry, University of Oxford, Oxford, OX1 3UB, England

Electron correlation plays an important role in determining the properties of physical systems, from atoms and molecules to condensed phases. Recent theoretical progress in the field has proven possible using both analytical methods and numerical many-body treatments, for realistic systems as well as for simplified models. Within the models, one may mention the jellium and the Hubbard. The jellium model, while providing a simple, rough approximation to conduction electrons in metals, also constitutes a key ingredient in the treatment of electrons in condensed phases within density-functional formalism. The Hubbard- and the related Heisenberg-model Hamiltonians, on the other hand, are designed to treat situations in which very strong correlations tend to bring about site localization of electrons. The character of the interactions in these lattice models allows for a local treatment of correlations. This is achieved by the use of projection techniques that were first proposed by Gutzwiller for the multicenter problem, being the natural extension of the Coulson-Fischer treatment of the H_2 molecule. Much work in this area is analytic or semianalytic and requires approximations. However, a full many-body treatment of both realistic and simplified models is possible by resorting to numerical simulations, i.e., to the so-called quantum Monte Carlo method. This method, which can be implemented in a number of ways, has been applied to atoms, molecules, and solids. In spite of continuing progress, technical problems still remain. Thus one may mention the fermion sign problem and the increase in computational time with the nuclear charge in atomic and related situations. Still, this method provides, to date, one of the most accurate ways to calculate correlation energies, both in atomic and in multicenter problems.

CONTENTS

I. INTRODUCTION

In this review, we shall consider some aspects of electron correlation in molecules and solids on which recent progress has proven possible. It is natural enough to start with the homogeneous electron fluid: i.e., the so-called jellium model of a metal, in which electrons interacting Coulombically move in a nonresponsive uniform, positive neutralizing background charge. Here, the ground-state energy is simply a function of the mean density $\rho_0=3/4\pi r_s^3 a_0^3$; $a_0=\hbar^2/me^2$. The pair correlations in this system are by now relatively well understood, as is the transition from a strongly correlated electron liquid to an insulating Wigner electron crystal at a suitable low value of the density, i.e., at large enough r_s. This is a spectacular manifestation of the effects of correlation. Only in the last decade have quantum Monte Carlo (QMC) simulations largely settled the critical value of r_s for this transition, placing it at about 100. Some attention will be given to such QMC results in Sec. IV of the present article, where correlation energies for small molecules, as well as numerical solutions of Hubbard and Heisenberg Hamiltonians, will also be referred to.

The jellium model affords the basis for the so-called theory of the inhomogeneous electron gas, which had its origin in the Thomas-Fermi method. This latter theory was formally completed by the Hohenberg-Kohn theorem (1964), which states that the ground-state energy of an inhomogeneous electron gas in a unique functional of its electron density $\rho(\mathbf{r})$. However, the functional is not yet known. There are fairly recent reviews both on

 0034-6861/94/66(2)/445(35)/$08.50

the electron gas (Singwi and Tosi, 1981; Ichimaru, 1982) and on the so-called density-functional theory (Bamzai and Deb, 1981; Ghosh and Deb, 1982; Lundqvist and March, 1983; Callaway and March, 1984; Jones and Gunnarsson, 1989; Parr and Yang, 1989). Thus we shall keep this discussion relatively short, focusing on the way Wigner electron crystallization can be treated within the density-functional framework. It is relevant in this context to stress at the outset that, while density-functional theory reveals the way in which electron correlation enters the calculation of the single-particle density, there is no means within the formal framework for calculating the required functional describing correlation.

Section III is concerned with the multicenter problems of molecules and solids, and the qualitative aspects of electron correlation are first stressed by summarizing the idea behind the Coulson-Fischer (1949) wave function for the ground state of the H_2 molecule. This idea is then taken up in relation to the work of Gutzwiller (1963, 1964, 1965) on strongly correlated electrons in narrow energy bands. In this treatment, electron interactions are treated by means of the Hubbard U, which, by definition, is the energy required to place two electrons with antiparallel spin on the same site. As in the Coulson-Fischer treatment, one reduces the weight of the ionic configurations that are obtained by expanding out a single Slater determinant of Bloch wave functions.

Because of the current excitement concerning superconductivity, the relevance of the Hubbard Hamiltonian in providing a quantitative basis for the development of Pauling's ideas on the resonant valence-bond theory of metals is briefly summarized also within the context of Gutzwiller's method.

To this stage in the article, the main theoretical development is via largely analytical methods. However, as mentioned already, important progress in the calculation of correlation energy in multicenter problems has resulted from the development of quantum computer simulation, pioneered in general terms by Anderson (1975, 1976, 1980) and applied to jellium by Ceperley and Alder (1980). Important here is to input a trial wave function, transcending wherever possible a single Slater determinant. Briefly, one form of the QMC method starts from the time-dependent Schrödinger equation or the equivalent Bloch equation in imaginary time, in contrast to the methods used elsewhere in the article. The alternative approach works directly with the many-particle Green's function, depending on all electronic coordinates and on an energy parameter. The strengths and the weaknesses of these methods are assessed. As well as the jellium results already mentioned, the parallel development in calculating correlation energies in small molecules will also be described. At the time of writing, though there are still some technical problems, this computer simulation approach provides a very accurate way of calculating electronic correlation energies in multicenter problems. Some promising directions for future work are suggested in concluding the article.

II. HOMOGENEOUS ELECTRON ASSEMBLY

We now turn to the discussion of correlation in a model appropriate to simple metals. It will be useful to focus first on the electron assembly formed by the conduction electrons in a metal like *Na* or *K*. In these cases, there is a whole body of evidence that demonstrates the weakness of the electron-ion interaction. Therefore the jellium model, introduced initially by Sommerfeld long ago, where the ionic lattice is smeared out into a uniform neutralizing background of positive charge in which the correlated electronic motion takes place, affords a valuable starting point.

Electron correlation can be treated quantitatively in this jellium model by numerical means (see, e.g., Sec. IV.D) at all densities, including metallic ones. Approximate treatments, on the other hand, are simpler in the two limiting cases of very high and very low densities. Though at first the problem looks totally different from the molecular case (see especially Sec. III.A), there is, in fact, a close parallel in the sense that in the high-density limit a delocalized picture (cf. molecular orbitals) is correct while, in the low-density limit, electron localization (cf. valence bond theory) is again induced by strong Coulomb repulsion between electrons.

In the following we shall focus especially on the regime of extreme low densities, where the effects of correlation are dominant, leaving aside the range of high and metallic densities (see, e.g., Singwi and Tosi, 1981). Here we shall just recall that at high densities, i.e., for $r_s \to 0$, the kinetic energy dominates the potential energy and an independent-particle description provides a reasonable starting point to describe the electron assembly. In fact, a single plane-wave determinant of spin orbitals is a Hartree-Fock solution for the jellium model, yielding a homogeneous density distribution (see, e.g., March *et al.*, 1967) and an energy

$$\frac{E_{\rm HF}}{N} = \left[\frac{2.21}{r_s^2} - \frac{0.916}{r_s} \right] Ry \ . \tag{2.1}$$

Many-body perturbation on such a state, in which electrons are fully delocalized, yields an approximate estimate of the correlation energy E_c (Gell-Mann and Brueckner, 1957), defined as the difference between the true ground-state energy E_0 and its Hartree-Fock approximation $E_{\rm HF}$, i.e., $E_c = E_0 - E_{\rm HF}$.

A. Low-density Wigner electron crystal

Turning to the extreme low-density limit $r_s \to \infty$, Wigner (1934, 1938) pointed out that the above delocalized picture broke down completely, and once the potential energy became large compared with the kinetic energy, the electrons would then want to avoid each other maximally. He stressed that this situation would be achieved by electrons becoming localized on the sites of a lattice. He argued that one must find the stable lattice by minimizing the Madelung energy. Of the lattices so far

examined, the bcc lattice has the lowest Madelung term. This yields, for the electron bcc Wigner crystal, the energy

$$\lim_{r_s\to\infty}\frac{E}{N}=-\frac{1.792}{r_s}Ry\ , \tag{2.2}$$

which shows, by comparison with the Hartree-Fock plane-wave result (2.1), that this latter approximation is no longer of any physical utility, the energy being too high by a factor of about 2.

As the repulsive coupling between the electrons is relaxed, that is, r_s reduced below the range of validity of Eq. (2.2), the electrons will vibrate about the bcc lattice sites. Since the bcc lattice has a Wigner-Seitz cell of high symmetry, it is a useful first approximation to neglect the (multipole) fields of the other cells in considering the vibration of an electron in its own cell. Then the potential energy $V(r)$, in which the electron vibrates, is created solely by the uniform positive background in its own cell, which, in the spherical approximation, gives

$$V(r)=\frac{e^2r^2}{2r_s^3a_0^3}+\text{const} \tag{2.3}$$

with the ground-state isotropic harmonic-oscillator wave function as

$$\psi(r)=\left[\frac{\alpha}{\pi}\right]^{3/4}\exp(-\tfrac{1}{2}\alpha r^2),\quad \alpha=(r_sa_0)^{-3/2}\ . \tag{2.4}$$

This Wigner oscillator leads to a kinetic energy per electron in the low-density limit as

$$\lim_{r_s\to\infty}\frac{T}{N}=\frac{3}{2r_s^{3/2}}Ry\ . \tag{2.5}$$

This is qualitatively different from the independent electron result $(2.21/r_s^2)Ry$. In fact, an obvious effect of switching on the electron-electron interaction away from the $r_s\to 0$ limit is to promote electrons outside the Fermi sphere of radius k_F, leaving holes inside (cf. Fig. 3). This creation of electron-hole pairs obviously increases the kinetic energy. Thus, if one writes $T/N=K/r_s^2$, the increase in kinetic energy appears as an increase in $K(r_s)$. In the limit $r_s\to\infty$, the creation of particle-hole pairs is so prolific that K diverges as $r_s^{1/2}$ and the Fermi sphere picture breaks down completely. The calculation yielding Eq. (2.5) is an Einstein-type model, whereas one should, of course, treat the vibrational modes of the bcc Wigner crystal by collective phonon theory. The coefficient 3 in Eq. (2.5) is then reduced to 2.66 (Carr, 1961; Coldwell-Horsfall and Maradudin, 1963).

The Fermi distribution is then profoundly altered by the creation of particle-hole pairs, and another way of seeing this is to take the Fourier transform of the Gaussian orbital (2.4), which, of course, yields also a Gaussian momentum distribution. At most, remnants of a Fermi surface remain in the low-density limit [in one dimension, this statement is made quantitative by Holas and March (1991)].

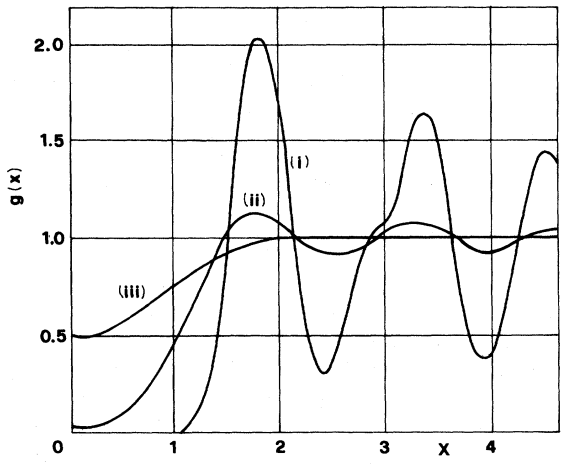

FIG. 1. Pair-correlation function $g(r)$ vs $x=r/r_sa_0$, for different densities: (i) Wigner form for $r_s=100$; (ii) Wigner form for $r_s=10$; (iii) Fermi hole, correct in the limit $r_s\to 0$.

A measure of the order present in a many-body system is afforded by the so-called pair-correlation function $g(r)$. This gives the probability of finding pairs of electrons at distance r. In the Wigner-crystal regime, and within the approximate framework of electrons behaving like Einstein oscillators, it is a straightforward matter to construct $g(r)$. Results for different values of r_s are shown in Fig. 1, taken from the work of March and Young (1959). The tendency of electrons to avoid each other with increasing r_s is apparent, as well as the greater amount of order present in the state in which the electrons are localized in Gaussian orbitals in contrast to that in which they are in plane waves.

B. Density-functional theory of many-electron system

One approach to incorporate, approximately, of course, electron correlation is afforded by the density-functional theory. However, because of related recent reviews (Lundqvist and March, 1983; Callaway and March, 1984; Jones and Gunnarsson, 1989) and books (see, e.g., Parr and Yang, 1989), our treatment will be very brief, merely to establish the notation and recall a few facts.

The theory has developed from the pioneering work of Thomas (1926) and Fermi (1928) and Dirac (1930), with a later paper by Slater (1951) also being very important in developing the present form of the density-functional theory. The step that was lacking, namely, the proof that the ground-state energy of a many-electron system is indeed a unique functional of the electron density, was taken by Hohenberg and Kohn (1964), who supplied the proof for a nondegenerate ground state.

It has proven helpful in developing the theory to separate the energy functional into a number of parts, closely paralleling the energy principle of the original Thomas-Fermi theory (cf. March, 1975).

Thus one writes the total energy $E[\rho]$ as a sum of an independent-particle kinetic-energy functional $T_s[\rho]$, electrostatic potential-energy terms, and then a contribution $E_{xc}[\rho]$ from exchange and correlation which are usefully considered together. Explicitly, we write

$$E[\rho]=T_s[\rho]+\int\rho(\mathbf{r})v(\mathbf{r})d\mathbf{r}+\frac{e^2}{2}\int\frac{\rho(\mathbf{r})\rho(\mathbf{r}')}{|\mathbf{r}-\mathbf{r}'|}d\mathbf{r}d\mathbf{r}'+E_{xc}[\rho]\ , \tag{2.6}$$

where $v(\mathbf{r})$ is the external potential acting on the electrons ($-Ze^2/r$ in an atom).

According to Hohenberg and Kohn (1964), $E[\rho]$ is a minimum at the equilibrium density distribution in the given external potential $v(\mathbf{r})$. Thus one minimizes this total energy with respect to the ground-state electron density $\rho(\mathbf{r})$, subject only to the condition that the electron density satisfy the normalization condition

$$\int\rho(\mathbf{r})d\mathbf{r}=N\ , \tag{2.7}$$

for a system with N electrons.

With the introduction of a Lagrange multipler μ, which has the significance of the chemical potential of the electron cloud of the atom, molecule, or solid being considered, the Euler equation of the variational problem reads

$$\mu=\frac{\delta T_s}{\delta\rho(\mathbf{r})}+v(\mathbf{r})+e^2\int\frac{\rho(\mathbf{r}')}{|\mathbf{r}-\mathbf{r}'|}d\mathbf{r}'+\frac{\delta E_{xc}}{\delta\rho(\mathbf{r})}\ , \tag{2.8}$$

which evidently expresses the constant chemical potential μ throughout the charge distribution as a sum of various contributions which vary from point to point, arising from kinetic, electrostatic, and exchange-plus-correlation contributions. In this form, as Kohn and Sham (1965) emphasized, thereby formally completing the treatment of Slater (1951), one can interpret the problem as posed in terms of equivalent independent-particle equations, which then bypasses the fact that even the independent-particle kinetic-energy functional is still not known in closed form [as a functional of $\rho(\mathbf{r})$]. Thus by solving single-particle Schrödinger equations, with a total one-body potential energy given by

$$v_{\text{eff}}(\mathbf{r})=v(\mathbf{r})+e^2\int\frac{\rho(\mathbf{r}')}{|\mathbf{r}-\mathbf{r}'|}d\mathbf{r}'+\frac{\delta E_{xc}}{\delta\rho(\mathbf{r})}\ , \tag{2.9}$$

one can avoid any approximation in the independent-particle kinetic energy. Furthermore, the above argument suggests that, in principle, the exact many-electron problem of calculating the ground-state electron density $\rho(\mathbf{r})$ can be reduced to a one-body problem (but see Parr and Yang, 1989, for a discussion of the subtleties of the so-called v representability). Naturally, the many-electron effects in the correlation energy functional are now subsumed in the one-body potential energy $v_{\text{eff}}(\mathbf{r})$, through the functional derivative $\delta E_{xc}/\delta\rho(\mathbf{r})$. Of course, exact knowledge of this quantity would require exact solution of the many-electron problem, which is currently not feasible. Extraction of the potential $v_{\text{eff}}(\mathbf{r})$ directly from the ground-state density has proved possible for the Be atom, however (Hunter and March, 1989).

C. Local-density approximations to exchange and correlation

As the simplest example of the use of Eq. (2.9), let us derive the so-called Dirac-Slater exchange potential. Here one neglects correlation and approximates the exchange energy density by its value in a uniform electron gas with its local density inserted at the point in question. This leads to the result that the total exchange energy, A, say, in Dirac-Slater approximation is given by

$$A=-c_e\int\rho(\mathbf{r})^{4/3}d\mathbf{r},\quad c_e=\frac{3e^2}{4}\left[\frac{3}{\pi}\right]^{1/3}\ . \tag{2.10}$$

Taking the functional derivative required by Eq. (2.9) leads immediately to the Dirac-Slater exchange potential

$$v_{\text{Dirac-Slater}}(\mathbf{r})=-\tfrac{4}{3}c_e\rho(\mathbf{r})^{1/3}\ . \tag{2.11}$$

This local-density approximation (LDA) has proved very valuable. In fact, one can extend it to treat the full exchange-correlation functional by setting

$$E_{xc}^{\text{LDA}}[\rho]=\int\epsilon_{xc}(\rho(\mathbf{r}))d\mathbf{r}\ . \tag{2.12}$$

Above, $\epsilon_{xc}(\rho_0)$ is the exchange-correlation energy per particle of the electron fluid at uniform density ρ_0, which is accurately known (cf., Sec. IV.D) and suitably parametrized (Vosko *et al.*, 1980; Perdew and Zunger, 1981).

It turns out that in the few examples that can be solved for the exchange energy, the Dirac-Slater form is a very useful approximation (see, however, Overhauser, 1985). For example, Miglio *et al.* (1981) have shown, in the case of the infinite barrier model of a metal surface, that although the electron density varies strongly at the surface, nevertheless the local-exchange theory discussed above remains a remarkably useful approximation.

The local-density approximation and its local spin-density extension have been widely applied, going all the way from atoms and molecules to clusters and solids. There are successes (many) and failures (not negligible ones), depending both on the physical quantity under consideration and on the class of systems. An up-to-date survey of the overall situation was given recently by Jones and Gunnarsson (1989). Modifications of the LDA schemes that go beyond the local dependence in Eq. (2.12), seek to include in the exchange and correlation functional additional information on the behavior of the single-particle density and/or to enforce exact limiting behaviors of the resulting exchange-correlation potential (see, e.g., Becke, 1992 and Johnson *et al.*, 1993). Of the many situations where the above theory, based as it is on using uniform electron-gas relations locally, is too crude, the electron Wigner crystal at zero temperature, i.e., in the fully degenerate limit, constitutes a good example.

D. Density-functional treatment of Wigner crystallization

Underlying the LDA of Eq. (2.12) is the assumption that one is concerned with systems with modulations of the electronic density which are neither too large nor too rapidly varying. In fact, LDA is commonly used in situations where the density is far from satisfying such requirements. Nonetheless, it is not surprising that LDA should perform poorly, especially in the treatment of the Wigner crystal mentioned in Sec. II.A, since this is characterized by both a strongly localized density and a crucial role of correlations. Below, we summarize in some detail the application to the study of the Wigner crystal of an approximation scheme that transcends LDA. However, before doing so, we anticipate that the most accurate assessment of the freezing density in jellium, $r_s = 100 \pm 20$, comes from quantum Monte Carlo simulations (cf. Sec. IV.D), which also establish that the transition to a bcc regular structure takes place from a fully spin-polarized liquid, this phase being lower in energy with respect to the unpolarized liquid for $r_s > 75$. Therefore in the following we shall content ourselves with a discussion of the coexistence between the spin-polarized liquid and a regular crystalline phase.

Senatore and Pastore (1990) find that the application of the LDA to the freezing of the spin-polarized electron fluid into a bcc crystal yields an exceedingly low value for the freezing density, $r_s = 22$. Hence they propose an approximation for exchange and correlation in which, rather than on the full functional $E_{xc}[\rho]$, one focuses on the difference $\Delta = E_{xc}[\rho_s] - E_{xc}[\rho_0]$ between the solid and the liquid phase and then resorts to an expansion of Δ about the liquid, in powers of the density difference $\rho_Q(\mathbf{r}) = \rho_s(\mathbf{r}) - \rho_0$. To second order, such an expansion yields

$$E_{xc}[\rho_s] = E_{xc}[\rho_0] + \frac{1}{2}\int\int d\mathbf{r}\, d\mathbf{r}' [-\chi^{-1}(\mathbf{r}-\mathbf{r}') + \chi_0^{-1}(\mathbf{r}-\mathbf{r}')]\rho_Q(\mathbf{r})\rho_Q(\mathbf{r}') , \tag{2.13}$$

with $\chi(r)$ and $\chi_0(r)$ being, respectively, the static response function of the homogeneous liquid and the response function of the noninteracting electrons (i.e., the Lindhard function). One of the motivations for using such a quadratic approximation is that, for classical liquids, it is known to work surprisingly well (for a recent review, see Baus, 1990).

As we mentioned in Sec. II.B, the Euler-Lagrange problem for the ground-state energy functional of interacting particles can be conveniently recast into the so-called Kohn-Sham problem (i.e., the self-consistent problem of noninteracting particles in a density-dependent one-body potential). Once the exchange-correlation functional is known, it is a simple matter to obtain at once the density-dependent Kohn-Sham potential. From Eqs. (2.9) and (2.13) one gets, in Fourier transform,

$$v_{\text{eff}}(\mathbf{q}) = \rho_Q(\mathbf{q})[-\chi^{-1}(q) + \chi_0^{-1}(q)] . \tag{2.14}$$

It may be worth stressing at this point that, whereas the LDA borrows only a thermodynamic property of the homogeneous liquid (i.e., the exchange-correlation energy), the quadratic approximation involves—in principle—structural information of the liquid at all the wave vectors which are relevant in the modulated phase. Thus, for a regular solid, one finds that such a region of wave vectors extends from about $2q_F$ onward.

To perform calculations, one needs the response function of the homogeneous interacting-electron liquid. This quantity, however, is not exactly known. Senatore and Pastore have therefore employed the so-called STLS (Singwi, Tosi, Land, Sjölander) decoupling scheme (Singwi *et al.*, 1968) to construct $\chi^{-1}(q)$ from the structure factor $S(k)$ obtained from the QMC simulations.

The calculation of the ground-state energy of the Wigner crystal requires the self-consistent solution of Kohn-Sham equations for the Bloch orbitals of a single fully occupied energy band, since there is one electron per unit cell and one is considering the spin-polarized state. This can be accomplished by using standard computational techniques for band-structure calculations. The results that are obtained can be summarized as follows.

The quadratic approximation predicts freezing into the bcc lattice at $r_s = 102$, a value which compares extremely well with the QMC prediction of $r_s = 100 \pm 20$. In addition, a Lindemann ratio γ (rms deviation about the lattice site divided by the nearest-neighbor distance) of 0.34 is obtained, whereas QMC suggests $\gamma = 0.30 \pm 0.02$ for all quantum systems studied to date. The calculated density still turns out to be well localized, even if considerably less so than in classical freezing. This, together with the high symmetry of the periodic structure, suggests the possibility of a tight-binding approximation in which Bloch orbitals are built from one Gaussian orbital per site with a variational width. Using this approximation, calculations simplify considerably, whereas the results for the freezing r_s and γ change only slightly. In fact, one gets $r_s = 107$ and $\gamma = 0.29$.

Senatore and Pastore have also investigated the stability of the fcc electron crystal. They find, within the fuller calculations, that the fcc solid is, in fact, the stable phase between $r_s = 97$ and $r_s = 108$, being in this range lower in energy than the bcc crystal (and, of course, also lower in energy than the homogeneous liquid). For higher values of the coupling r_s, the bcc remains the stable phase, in agreement with the findings of harmonic lattice calculations (see, e.g., Foldy, 1971).

An investigation of the importance of higher-order

terms in the expansion of Eq. (2.13), when applied to the study of Wigner crystallization, was subsequently conducted by Moroni and Senatore (1991), who resorted to density-functional-theory schemes of the weighted-density type. While there are quantitative changes in the details of the freezing transition, the agreement with the QMC results remains very good. One should note that the freezing theory summarized above crucially relies on the knowledge of the static response function of the quantum liquid. The sensitivity of the results to the accuracy with which $\chi(q)$ is known is thus an important issue. At present there is little knowledge about the precise form of static response in quantum fluids. However, some progress has recently been made for the two-dimensional electron gas and for ^{4}He (Moroni *et al.*, 1992), using QMC techniques, and, in fact, work using similar means is in progress on the three-dimensional electron fluid (Moroni *et al.*, 1993).

III. LOCALIZED VERSUS MOLECULAR-ORBITAL THEORIES OF ELECTRONS IN MULTICENTER PROBLEMS: GUTZWILLER VARIATIONAL METHOD

We begin by stressing that one-center (i.e., atomic) correlation effects have to be treated by quantitative examination of the problem, except for isolated instances of collective effects within specific shells (see, for example, Wendin, 1986). In contrast, as already mentioned, we have qualitative consequences in multicenter problems, which are worthy of full consideration. Let us start by reviewing the situation in the H_2 molecule, going back to the pioneering work on the chemical bond by Heitler and London (1927).

This Heitler-London description merely asserted that a useful ground-state symmetric space wave function could be built up from the atomic orbitals (1*s* functions) centered on nuclei *a* and *b*, namely, ϕ_a and ϕ_b. After symmetrization, one is led to the wave function

$$\Psi_{\rm HL}(1,2)=\phi_a(1)\phi_b(2)+\phi_b(1)\phi_a(2)\ . \tag{3.1}$$

The first term on the right-hand side of Eq. (3.1) evidently corresponds to electron 1 on nucleus *a* and electron 2 on nucleus *b*. The second part is added because of the indistinguishability of electrons.

Turning to the delocalized description, one introduces a molecular orbital $\psi_{\rm MO}$, and, in the singlet ground state, one puts two electrons into it with opposed spins. Then the MO total space wave function is written in the form

$$\Psi_{\rm MO}(1,2)=\psi_{\rm MO}(1)\psi_{\rm MO}(2) \tag{3.2}$$

and, in terms of the 1*s* atomic orbitals, in the approximation in which the molecular orbital is built up as a linear combination of atomic orbitals,

$$\begin{aligned}\Psi_{\rm LCAO\text{-}MO}(1,2)&=[\phi_a(1)+\phi_b(1)][\phi_a(2)+\phi_b(2)]\\&=\Psi_{\rm HL}(1,2)+\phi_a(1)\phi_a(2)+\phi_b(1)\phi_b(2)\ .\end{aligned} \tag{3.3}$$

In the second part of Eq. (3.3), we have noted explicitly that the LCAO-MO wave function can be viewed as a linear superposition of the Heitler-London covalent terms and an equally weighted admixture of ionic terms, $\phi_a(1)\phi_a(2)$ evidently representing both electrons on nucleus *a*, etc. That Eq. (3.3) is incorrect as the internuclear distance *R* gets large compared with the size a_0 of the 1*s* hydrogen orbitals is quite clear; the molecule dissociates into two neutral H atoms, just as described by the original Heitler-London wave function (3.1).

A. Coulson-Fischer wave function with asymmetric orbitals, for H_2 molecule

An important clarification of the role of electron correlation in molecules came with the work of Coulson and Fischer (1949) on H_2. They asked the question as to what was the best admixture of covalent and ionic states at each internuclear distance *R*, by contemplating asymmetric molecular orbitals $\phi_a+\lambda\phi_b$, $\lambda\leq 1$, and $\phi_b+\lambda\phi_a$, the former representing, with $\lambda<1$, the electron primarily but not wholly belonging to nucleus *a*, etc. Then they formed the (unsymmetrized) variational wave function

$$\Psi_{\rm Coulson\text{-}Fischer}=[\phi_a(1)+\lambda\phi_b(1)][\phi_b(2)+\lambda\phi_a(2)]\ . \tag{3.4}$$

Determining λ as a function of *R* by minimization of $\langle H\rangle$ with respect to the wave function (3.4), *H* being the total Hamiltonian of the H_2 molecule, they found the following situation: (a) for $R<1.6R_{\rm equilibrium}$, $\lambda=1$; (b) for $R>1.6R_{\rm equilibrium}$, λ falls quite rapidly to zero as *R* is increased. $R_{\rm equilibrium}$ being the equilibrium internuclear separation. For $\lambda=1$, Eq. (3.4) becomes identical with Eq. (3.3), whereas for $R>1.6R_{\rm equilibrium}$ we see that electrons quickly "go back on to their own atoms."

This idea, that one decreases the weight of the ionic configurations in a molecular-orbital treatment, has been taken up in the work of Gutzwiller (1963, 1964, 1965) for treating strong correlations in narrow energy bands, and we shall discuss the results of his method in some detail below.

The important point to be stressed from the above is that electron correlations can have the qualitative effect of driving electrons back on to their own atoms when the internuclear spacing becomes substantially larger than the size of the atomic orbitals involved.

It is convenient at this point to follow Falicov and Harris (1969) and refer to a model for a two-electron homopolar molecule. These workers discuss the eigenstates of the one-band Hamiltonian for such a two-electron system, and their results are summarized in Appendix A. They then use the exact solution for the ground state as a standard to assess the validity of the MO, Heitler-London and other states having either spin- or charge-density waves.

By definition, of course, the MO approximation is undercorrelated, the Heitler-London states being always

overcorrelated. The spin-density and charge-density waves are less easily classified, with the question of under- or overcorrelated depending on the strength of the interaction.

Falicov and Harris construct from spin- and charge-density-wave states, which have broken symmetry, symmetrized versions. These symmetrical states were always found in their work to be slightly undercorrelated. This work has been extended by Huang *et al.* (1976).

B. Gutzwiller's variational method

As mentioned above, a possible way to account for correlation of antiparallel electrons in a multicenter problem is to partly project out from a given uncorrelated wave function those components corresponding to double occupied (ionic) sites. In the simple case of H_2, this was most simply done by Coulson and Fischer (1949) as set out in Sec. III.A. The generalization of such an approach to situations with an arbitrary number of centers is due to Gutzwiller (1963, 1965). Here we shall just outline the key points of Gutzwiller's approach, which has been reviewed by Vollhardt (1984). In the next two sections, we shall discuss in some detail the application of the Gutzwiller variational method to treat the correlation in molecules, on the one hand, and the Hubbard Hamiltonian, on the other. The latter has received renewed attention in connection with the exciting discovery of high-T_c superconductivity (Bednorz and Müller, 1986).

The starting point of Gutzwiller's variational approach is the uncorrelated wave function, for the problem under consideration. This is constructed, for a regular lattice with N sites and one Wannier orbital ϕ per site, from the Bloch waves $\Psi_{\mathbf{k}}(\mathbf{r})$,

$$\Psi_{\mathbf{k}}(\mathbf{r})=\frac{1}{\sqrt{N}}\sum_i \exp(i\mathbf{k}\mathbf{R}_i)\phi(\mathbf{r}-\mathbf{R}_i)\ . \tag{3.5}$$

Using the second-quantization formalism, the uncorrelated ground-state wave function can be written as

$$|\Phi_0\rangle=\prod_{\mathbf{k}\in K} a^\dagger_{\mathbf{k}\uparrow}\prod_{\mathbf{q}\in Q} a^\dagger_{\mathbf{q}\downarrow}|0\rangle\ , \tag{3.6}$$

where $a^\dagger_{\mathbf{k}\sigma}$ is the creation operator of an electron in the Bloch wave $\Psi_{\mathbf{k}}$ and with spin projection σ, $|0\rangle$ is the vacuum state, and K and Q are sets of points in reciprocal space, which in general may be delimited by different Fermi surfaces. If one denotes the creation operator of an electron in the Wannier orbital ϕ at the site i by $a^\dagger_{i\sigma}$,

$$a^\dagger_{i\sigma}=\frac{1}{\sqrt{N}}\sum_{\mathbf{k}}\exp(-i\mathbf{k}\mathbf{R}_i)a^\dagger_{\mathbf{k}\sigma}\ , \tag{3.7}$$

and the corresponding number operator by $n_{i\sigma}$, the Gutzwiller wave function can be written as

$$|\Phi\rangle=\prod_i[1-(1-g)n_{i\uparrow}n_{i\downarrow}]|\Phi_0\rangle=g^D|\Phi_0\rangle\ . \tag{3.8}$$

Above, $D=\sum_i n_{i\uparrow}n_{i\downarrow}$ is the operator that counts the number of double occupied sites. Clearly, in the wave function Φ, the components containing double occupied sites are reduced by a fractional amount $1-g$ $(0\le g\le 1)$ with respect to their value in the uncorrelated wave function Φ_0, thus reducing the repulsive interaction energy among antiparallel electrons. For a given Hamiltonian H, the variational parameter g has to be determined by minimizing the ground-state energy

$$E_0(g)=\frac{\langle\Phi|H|\Phi\rangle}{\langle\Phi|\Phi\rangle}\ . \tag{3.9}$$

To fix ideas, let us briefly consider the case originally investigated by Gutzwiller, that of the so-called Hubbard Hamiltonian,

$$H=\sum_{ij}\sum_\sigma t_{ij}a^\dagger_{i\sigma}a_{j\sigma}+U\sum_i n_{i\uparrow}n_{i\downarrow}\ , \tag{3.10}$$

which is designed to describe fermions on a lattice in a narrow-band system. The first term on the right-hand side of Eq. (3.10) is the kinetic energy due to the hopping of electrons between sites, and the second one crudely describes the on-site repulsion of antiparallel-spin electrons. It is straightforward to show that for $g=1$ one simply regains the uncorrelated state, which of course is the exact ground state for zero on-site repulsion, $U=0$. In this case $D=D_0\equiv N_\uparrow N_\downarrow/N$. On the other hand, $g=0$ corresponds to a fully correlated wave function in which the components containing double occupied sites are suppressed and $D=0$. This is the exact ground state for $U=\infty$. Therefore, for finite repulsion, one will have $0<g<1$ and $0<D<D_0$, since the effect of correlation is precisely to reduce the number of doubly occupied sites present in the uncorrelated wave function.

Thus far, even for the Hubbard Hamiltonian, the evaluation of the averages in Eq. (3.9) has proved too difficult to carry out analytically in the general case, with the notable exception of the one-dimensional lattice (Gebhard and Vollhardt, 1987; Metzner and Vollhardt, 1987). Hence one has either to employ numerical methods (Horsch and Kaplan, 1983; Gros *et al.*, 1987a, 1987b; Yokoyama and Shiba, 1987a, 1987b) or to resort to approximate treatments, as originally done by Gutzwiller (1963, 1965). It has subsequently been shown that the approximations originally introduced by Gutzwiller to evaluate the averages in Eq. (3.9) are just equivalent to the neglect of the spin-configuration dependence of the various terms appearing in the expansion of both $\langle\phi|H|\phi\rangle$ and $\langle\phi|\phi\rangle$ (Ogawa *et al.*, 1975; see also Vollhardt, 1984). While the interested reader is urged to consult the original papers for the details of Gutzwiller's approximation (GA), it is convenient to report here at least the main results of GA as applied to the Hubbard Hamiltonian.

Within the GA, the average of Eq. (3.9) with the Hamiltonian given in (3.10) can be written as

$$E_0/N=n_\uparrow q_\uparrow\bar{\epsilon}_\uparrow+n_\downarrow q_\downarrow\bar{\epsilon}_\downarrow+Ud\ . \tag{3.11}$$

Here, $n_\sigma=N_\sigma/N$; q_σ is the discontinuity of the momen-

tum distribution $n_{\mathbf{k}\sigma}$ at the Fermi surface; $d=D/N$, with D the average number of double occupied sites; and

$$\bar{\epsilon}_\sigma=\frac{1}{N_\sigma}\sum_{|\mathbf{k}|<k_{F\sigma}}\epsilon(\mathbf{k})\ . \tag{3.12}$$

In Eq. (3.12), $\epsilon(\mathbf{k})$ is the energy eigenvalue of the Bloch wave $\Psi_{\mathbf{k}}$,

$$\epsilon(\mathbf{k})=\frac{1}{N}\sum_{ij}t_{ij}\exp[-i\mathbf{k}(\mathbf{R}_i-\mathbf{R}_j)]\ , \tag{3.13}$$

and the zero of energy has been chosen so that $\sum_{\mathbf{k}}\epsilon(\mathbf{k})=0$; i.e., $t_{ii}=0$. The GA simply yields

$$q_\sigma=\frac{\{[(n_\sigma-d)(1-n_\sigma-n_{-\sigma}+d)]^{1/2}+[(n_{-\sigma}-d)d]^{1/2}\}^2}{n_\sigma(1-n_{-\sigma})}\ , \tag{3.14}$$

where g has been eliminated in favor of d, and d has to be determined variationally, by minimizing the ground-state energy $E_0(d)$ as given in Eq. (3.11). In the special case of a paramagnetic half-filled band, for which $n_\uparrow=n_\downarrow=1/2$, $q_\uparrow=q_\downarrow=q$, and $\bar{\epsilon}_\uparrow=\bar{\epsilon}_\downarrow=\bar{\epsilon}_0<0$, one obtains, after minimization,

$$d=\frac{1}{4}\left[1-\frac{U}{U_c}\right]\ , \tag{3.15}$$

$$q=1-\left[\frac{U}{U_c}\right]^2\ , \tag{3.16}$$

$$E_0/N=|\bar{\epsilon}_0|\left[1-\frac{U}{U_c}\right]^2\ , \tag{3.17}$$

with $U_c=8|\bar{\epsilon}_0|$. This shows that, within the GA, at a finite critical value of the interaction $U=U_c$, d, q, and E_0 all vanish. The vanishing of the discontinuity in the momentum distribution at the Fermi surface, and consequently of the kinetic energy, would signal a metal-insulator transition (Brinkman and Rice, 1970; see also March *et al.*, 1979 and March and Parrinello, 1982). In fact, at the critical strength U_c, all sites would be singly occupied and the particles fully localized. We shall return to this point below.

Before turning to the discussion of how the Gutzwiller variational method has been generalized to treat interatomic and intra-atomic correlation in molecules, we have to mention more recent work by Kotliar and Ruckenstein (1986). These authors have proposed a new treatment of the Hubbard Hamiltonian that makes use of auxiliary boson fields, in analogy with the so-called *slave-boson* approach first proposed by Barnes (1976). They have shown that, within the functional-integral formalism, a particular choice of the auxiliary fields yields exactly the result of GA, as a mean-field or, more precisely, a saddle-point approximation to the exact functional integral. The merit of such an approach is that in principle it would allow for systematic improvement upon GA, in that one could study the effect of Gaussian fluctuations about the saddle point. However, nothing has been done in this direction, to our knowledge, at the time of writing.

C. Local approach to correlation in molecules

As we have discussed above, the local approach to correlation was introduced by Coulson and Fischer in the qualitative treatment of the H_2 molecule. Subsequently, Gutzwiller extended such an idea to solids to deal with strong correlation in narrow bands originating from very localized orbitals such as d orbitals, within the model description afforded by the Hubbard Hamiltonian. Starting from Gutzwiller's systematic scheme, a further step toward the quantitative treatment of correlation in small molecules was taken by Stollhoff and Fulde (1977, 1978).

Their main point is as follows. One still wants to set up a variational scheme in which those components of the wave functions that correspond to two electrons being too close are reduced. To this end, the wave function may be described, for instance, by assigning its value on the points of a spatial mesh (the grid) in which the system of interest, say, the molecule, is embedded. In practice, one may as well give at such points the amplitudes of basis-set functions, in terms of which the uncorrelated wave function is expanded. Within this picture, the wave function of Eq. (3.8) corresponds to a grid whose points coincide with the locations of atoms in the molecule. A quantitative treatment clearly requires that one improve upon the ansatz of Eq. (3.8) in at least two ways. One should (a) choose a finer grid, and (b) correlate the electronic motion not only on-site but also between different sites. The latter point can be easily realized by generalizing the variational wave function to read (Stollhoff and Fulde, 1977)

$$|\Phi\rangle=\prod_{i=0}^{I}P_i|\Phi_0\rangle\ , \tag{3.18}$$

where the P_i's are projection operators defined by

$$P_i=\prod_j(1-\eta_i 0_{ij})\ , \tag{3.19}$$

and

$$0_{0j}=n_{j\uparrow}n_{j\downarrow}\ , \tag{3.20}$$

$$0_{ij}=\sum_{\sigma\sigma'}n_{j\sigma}n_{j+i\sigma'}\ . \tag{3.21}$$

For $I=0$, Eq. (3.18) yields the original Gutzwiller ansatz. However, for nonzero I, density correlations between different grid points are also taken into account, up to the Ith neighboring points. Notice that, in the latter case, one is correlating also the motion of parallel-spin electrons on different grid points. The reason for this is that, though the uncorrelated wave function $|\Phi_0\rangle$ is antisym-

metrized, the Pauli exclusion principle is completely effective only at very short distances.

The problem of a finer grid can also be dealt with in quite a simple way (Stollhoff and Fulde, 1978). Instead of directly making the grid finer, one can alternatively choose to keep as grid points the atomic position in the molecule, while using at each site a number of basis-set functions with varying degrees of localization, possibly also off-center. Thus the operator $a_{i\sigma}^{\dagger}$ creates an electron in the basis-set function i rather than in one of the self-consistent one-particle orbitals in terms of which $|\Phi_0\rangle$ is constructed. Here, the index i labeling the creation operator stands, in fact, for the pair (i,α), where α indicates either one of the original basis-set functions or a suitable new combination; it might be, for instance, an s-p hybrid.

The effect of taking into account off-site correlation through the use of the variational wave function given in Eq. (3.18) with $I\neq 0$ has been investigated by Stollhoff and Fulde (1977) by studying the H_6 model of Mattheiss (1961). This model has the advantage that one knows the exact solution, which was obtained numerically. The model assumes six sites equally spaced on a ring, with one s atomic orbital at each site. From these, one constructs a Wannier orbital, in terms of which the Hamiltonian reads

$$H=\sum_{ij\sigma} t_{ij}a_{i\sigma}^{\dagger}a_{j\sigma}^{\dagger}+\sum_{\substack{ijkl\\ \sigma\sigma'}} V_{ijkl}a_{i\sigma}^{\dagger}a_{j\sigma'}^{\dagger}a_{l\sigma'}a_{k\sigma}\ . \tag{3.22}$$

Bloch waves are then built from the Wannier orbital, and from these the uncorrelated Hartree-Fock ground state $|\Phi_0\rangle$ is obtained. The correlation energy of the system was studied by Stollhoff and Fulde for various values of the first-neighbor distance R, with the variational wave function of Eq. (3.18). They found that the simpler Gutzwiller ansatz, i.e., $I=0$, only yields about 50% of the exact correlation energy at the exact equilibrium distance, $R=1.8$ a.u. On the other hand, the situation improves substantially by going to $I=1$, and even more for $I=2$. In the latter case, one recovers more than 95% of the correlation energy for any distance. The situation is illustrated in some detail in Fig. 2. It should also be noticed that a further increase of I from 2 to 3 does not produce anything new, since $I=3$ corresponds to the largest distance of the atoms in the ring.

Stollhoff and Fulde also investigated the accuracy of a simplified version of Eq. (3.18) obtained by linearization,

$$|\Phi\rangle=\left[1-\sum_{i=0}^{I}\eta_i\sum_j 0_{ij}\right]|\Phi_0\rangle\ , \tag{3.23}$$

in order to reduce computational complexity. With this simplified variational ansatz, they found that at the equilibrium distance about 90% of the correlation energy was still recovered with $I=2$. However, the agreement with the exact results becomes worse at larger distances, in contrast with the systematic improvement found with the full variational wave function of Eq. (3.18).

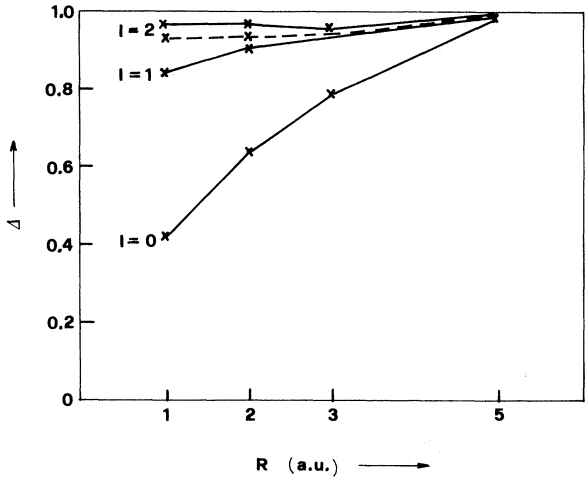

FIG. 2. Gain in correlation energy $\Delta=(E_{\rm HF}-E_{\rm Gutz.})/(E_{\rm HF}-E_{\rm exact})$ for the H_6 model by using the ansatz of Eq. (3.18) to evaluate the ground-state energy $E_{\rm Gutz.}$. Results are shown for $I=0$ to 2. The dashed line is the approximation given by Eq. (3.23). From Stollhoff and Fulde (1977).

It should be mentioned that, in general, using the linearized wave function of Eq. (3.23) to variationally calculate the correlation energy yields the so-called size-consistency problem. In practice the correlation energy does not turn out to be proportional to the electron number; i.e., it is not extensive as it should be in the limit of a large system. A way to restore the correct number dependence is to expand the variational ground-state energy of Eq. (3.9) to a given order in the variational parameters, say, the second, starting from the full wave function of Eq. (3.18). In the case of small molecules, the difference that one finds in correlation energy, with respect to the use of the linearized wave function (3.23), is only of a few percent (Stollhoff and Fulde, 1980). Another possible way to tackle the size-consistency problem begins with the rewriting of the product of projection operators appearing in Eq. (3.18) in an exponential form. This makes it possible to prove a linked-cluster theorem (see, for instance, Horsch and Fulde, 1979), which in turn allows a systematic expansion of the correlation energy in terms of connected diagrams. Again, the correct number dependence of the energy is automatically preserved to any order in the expansion in powers of the variational parameters. It should also be mentioned that spin-spin correlation can be dealt with as well, within the local approach. To this purpose one can just enlarge the class of projection operators appearing in Eq. (3.18) by defining further operators $0_{ij}=s_i\cdot s_j$, where s_i is the spin operator at the site i (Stollhoff and Fulde, 1978).

Clearly, in the study of the H_6 model only interatomic correlations could be taken into account, and admittedly within an oversimplified model. Therefore, for a more stringent test, Stollhoff and Fulde (1978, 1980) studied, within the simplified variational ansatz of Eq. (3.23),

some small atoms and molecules, taking into account intra-atomic correlations as well. To this end, the radial correlation was treated by considering basis-set functions of s type with different degrees of localization. On the other hand, angular correlations were introduced by using appropriate hybrid functions. In particular, s-p mixing was used to get sets of tetragonal hybrids, and d and f functions were used to obtain hybrids with hexagonal and octagonal symmetry, respectively. Within their simple scheme they were able to recover 93% of the experimental correlation energy for He and 90% for H_2. Thus, starting from the Hartree-Fock uncorrelated ground state, in both cases the results of the local approach based on a Gutzwiller-like ansatz yielded a fraction of the correlation energy, very close (a few percent of difference) to the one obtained in configuration-interaction (CI) calculations with the same basis sets. Similar results were also obtained for He_2 and Be.

A very detailed study of Ne and CH_4 along these lines (Stollhoff and Fulde, 1980) shows that also in more complex situations the local approach is capable of accounting for the correlation energy obtainable with CI calculations, within a few percent. One should notice, though, that the agreement with experiment of the correlation energy yielded by CI calculations with reasonable basis sets tends to worsen with increasing complexity of the system studied.

More recently, Oles *et al.* (1986) proposed another computational scheme for the treatment of correlations in more complex molecules containing C, N, and H atoms. While the interatomic correlations are still treated within a local approach based on semiempirical self-consistent-field calculations, intra-atomic correlations are dealt with by means of a different and simpler scheme. Good agreement is found with experimental results, discrepancies being within a few percent. They have also shown that simple algebraic parametrizations are possible for the various contributions to the correlation energy. In particular, interatomic correlations are found to depend only on bond lengths, whereas intra-atomic correlations are found to be determined for a given atom by its total charge and fraction of p electrons. A further study, on the determination of optimal local functions for the calculation of the correlation energy within the local approach, has also recently appeared (Dieterich and Fulde, 1987).

In the foregoing, we have been concerned with the application of a local approach to the calculation of correlation in molecules. Yet we should like to mention here an important development along these lines concerning extended systems. The above local approach, in fact, has been suitably modified (Horsch and Fulde, 1979) to treat also short-range and long-range correlation in the ground state of solids. A first attempt to calculate in this manner the correlation contribution to the ground-state energy of diamond (Kiel *et al.*, 1982) suffered the limitation of a poorly converged uncorrelated ground state. When an uncorrelated ground state of good quality is used, however, the local approach performs remarkably well, reproducing the electronic contribution to the binding energy of diamond with an accuracy of about 2% (Stollhoff and Bohnen, 1988).

D. Gutzwiller's variational treatment of the Hubbard model

As we have mentioned above, the Gutzwiller variational method was originally applied to the study of the so-called Hubbard model, characterized by the Hamiltonian of Eq. (3.10). In spite of the apparent simplicity of such a Hamiltonian, the relevant variational calculation is of considerable difficulty. Therefore Gutzwiller solved the problem in an approximate manner. It has been only recently, after some decades, that a renewed interest in this problem has brought about a certain amount of work leading to the exact solution of the variational problem, by direct numerical evaluation, by analytical means, or by the Monte Carlo method.

Kaplan, Horsch, and Fulde began a study in 1982 to assess the accuracy of the Gutzwiller variational wave function (GVW) in describing the ground state of the single-band Hubbard model with only nearest-neighbor hopping, in the atomic limit, i.e., the limit in which $U\rightarrow\infty$. In this case there is no variation to be taken. In fact, $g=0$, and the Gutzwiller wave function reads

$$|\Phi_\infty\rangle=\prod_i [1-n_{i\uparrow}n_{i\downarrow}]|\Phi_0\rangle \ . \tag{3.24}$$

They were able to perform, for the half-filled-band situation, the direct numerical evaluation of the spin-spin correlation function,

$$q_l=\langle s_i^z s_{i+l}^z\rangle \ , \tag{3.25}$$

for a number of small regular rings. The actual calculations were done for rings of 6, 10, 14, and 18 sites. By extrapolating from the results for finite rings, they found that in the thermodynamic limit (number of sites N going to infinity) $q_1=-0.1474$, thus being within 0.2% from the exact result, i.e., within the error bars of their calculation. For q_2, instead, the discrepancy with the exact result was of about 7%. They also noticed that the spin-spin correlations that they obtained reproduced as well qualitative features of the exact ones. Hence for large U, at least in one dimension, Gutzwiller's wave function describes the short-range spin-spin correlations in an accurate manner. We should notice here that, in the atomic limit and for the half-filled-band case, the exact ground state of the 1D Hubbard model is known to be the same as for the antiferromagnetic Heisenberg chain, for which q_1 was exactly evaluated by Bonner and Fisher (1964), and q_2 by Takahashi (1977). In fact, in the large-U limit, the Hubbard Hamiltonian goes, to leading order in t/U, into the Heisenberg Hamiltonian with antiferromagnetic coupling,

$$H=J\sum_{\langle ij\rangle}(\mathbf{s}_i\cdot\mathbf{s}_j-\tfrac{1}{4}) \ , \tag{3.26}$$

where J is proportional to t^2/U and t is the hopping energy. We shall return to this point in some detail.

Kaplan, Horsch, and Fulde also studied the energy for large but finite U. In this case one has to start from the full variational wave function (3.8) and consider an expansion of the energy in powers of the parameter g, to be determined variationally. They found that the leading term of such an expansion was of the form $E=-N\alpha t^2/U$, with α depending on the kinetic-energy operator and on the zero- and first-order wave functions obtained from the expansion of the variational wave function (3.8) in powers of g. Note that the zero-order wave function, which was given in Eq. (3.24), has no sites with double occupancy, as is clear by inspection. Similarly, the first-order one has on average only one site doubly occupied. They found that, at variance with the spin-spin correlations, the coefficient α yielded by the GVW was in gross disagreement with the known exact value. It is now known, from the exact solution of the Hubbard model in one dimension with the GVW (Metzner and Vollhardt, 1987), that α is not a constant, but vanishes as $1/\ln(U/t)$ in the limit considered by Kaplan, Horsch, and Fulde. These authors argued that the unsatisfactory result for the energy yielded by the GVW was due to the incorrect description of correlations between doubly occupied sites and empty sites, or holes, as we shall call them in the present context. Therefore they considered a modification of the GVW containing a second variational parameter to improve the treatment of such correlations. In this manner they were able to reproduce the exact value of α within 1%.

A further step toward the assessment of the reliability of the GVW was then taken by Horsch and Kaplan (1983). They extended the calculation for finite rings to other values of N, corresponding to open-shell systems, and also performed calculations for much larger systems with N up to 100 by using the Monte Carlo method to evaluate the relevant averages. This second step was particularly important. First, it fully confirmed the conclusions previously obtained from the exact calculations for small rings. Secondly, it was the first application of the Monte Carlo method to this problem. Before turning to the presentation of more recent studies on the Hubbard model, with a variational Monte Carlo technique based on the GVW, we shall summarize below the exact results that have been recently obtained in one dimension for arbitrary band filling and interaction strengths.

1. Exact analytic results in one dimension

Analytic results for the ground-state energy and momentum distribution function for the Hubbard model with on-site repulsion have been recently obtained by Metzner and Vollhardt (1987) for the paramagnetic situation. The key point of their attack on the problem at hand lies in a new approach to the calculation of the expectation values of relevant operators on the GVW.

The calculation of the ground-state energy appears to require the evaluation of the expectation values of both kinetic and potential energy for arbitrary values of the variational parameter g, $0\le g\le 1$. Let us start from the potential energy. It is clear from Eq. (3.10) that, apart from the proportionality constant U, the potential-energy operator is the same as the operator D that counts the number of doubly occupied sites. Thus one has to calculate $\langle D\rangle$ on the wave function of Eq. (3.8). Let us indicate the product $n_{i\uparrow}n_{i\downarrow}$ by D_i. It is then not difficult to show that

$$d=\frac{\langle D\rangle}{N}=g^2\sum_{m=1}^{\infty}(g^2-1)^{m-1}c_m\ , \tag{3.27}$$

where N is the number of sites, and the coefficients $c_m=x_m/N(m-1)!$ are suitable expectation values, which, if one puts $x_m=y_m/\langle\Phi|\Phi\rangle$, are explicitly given by

$$y_m=\sum_{f_1,\ldots,f_m}{}'\langle\Phi_0|D_{f_1}\cdots D_{f_m}|\Phi_0\rangle,\quad m\le N\ , \tag{3.28}$$

with $f_i\neq f_j$ (prime on sum). The expectation value appearing above can be transformed into the sum over all the possible pairs of contractions, $P_{ij}\equiv\langle a_{i\sigma}^{\dagger}a_{j\sigma}\rangle_0$, using Wick's theorem. We shall indicate such a sum by $\{\cdots\}_0$. The important point to realize is that, because of the prime on the sum in Eq. (3.28), one can choose to put $\langle a_{i\sigma}a_{j\sigma}^{\dagger}\rangle\equiv -P_{ji}$, since in this second kind of contraction one has always $i\neq j$ and therefore there is no δ_{ij} contribution. Equation (3.28) can then be rewritten as

$$y_m=\sum_{f_1,\ldots,f_m}{}'\{D_{f_1}\cdots D_{f_m}\}_0\ . \tag{3.29}$$

One can show that the sum $\{\cdots\}_0$ appearing above is, in fact, the determinant of a matrix having the P_{ij} as elements. Hence, for any $f_i=f_j$, the sum $\{\cdots\}_0$ vanishes, since the relative determinant has two identical rows. As a result, one has the freedom to remove the prime from the sum in Eq. (3.29). Having done so, one can next observe that in a diagrammatic analysis of x_m with lines corresponding to the P_{ij}, the contributions to $\{\cdots\}_0$ arising from disconnected diagrams just cancel the norm $\langle\Phi|\Phi\rangle$. Therefore one is left with

$$x_m=\sum_{f_1,\ldots,f_m}\{D_{f_1}\cdots D_{f_m}\}_0^c\ . \tag{3.30}$$

We notice that thus far no reference was made to interaction strength or to dimensionality.

While in the above the analysis was quite general, to date further progress has proved possible only in one dimension. In particular, in one dimension and for zero total spin ($n_\uparrow=n_\downarrow=n/2$), it is possible to show that c_m is proportional to n^{m+1}. One can restrict attention to $0\le n\le 1$, since, due to particle-hole symmetry for $1\le n\le 2$, the relation $d(n)=d(2-n)+n-1$ holds. By using the dependence of d on n and imposing the continuity of its first derivative, the proportionality constant in c_m can be calculated. One obtains

$$c_m = \tfrac{1}{2}(-1)^{m+1} n^{m+1}/(m+1) . \tag{3.31}$$

With the above equation for the coefficients c_m, the series in Eq. (3.27) is exactly summed to

$$d = \frac{n^2}{2}\left[\frac{g}{1-G^2}\right]^2\left[\ln\frac{1}{G^2}+G^2-1\right] , \tag{3.32}$$

with $G^2=1-n+ng^2$. We stress that, as is clear from Eq. (3.32), for the half-filled band—for which $n=1$—the correlation energy Ud is found to be nonanalytic in g, because of the presence of the term $\ln(1/g)$. For strong correlations ($g\to 0$), one finds $d=g^2\ln(1/g)$. Moreover, the double occupancy d is never vanishing for finite correlations, in contrast with the GA result of Eq. (3.15). This seems to be the case also in two and three dimensions when the GVW is exactly handled (Yokoyama and Shiba, 1987a).

A similar, though more complicated, analysis allows the calculation of the momentum distribution function for the same situation considered immediately above, i.e., $n_\uparrow = n_\downarrow = n/2$. We shall content ourselves here with quoting just the result for the discontinuity q in the momentum distribution function $n_{k\sigma}$,

$$q = G^{-1}[(G+g)/(1+g)]^2 . \tag{3.33}$$

The overall shape of $n_{k\sigma}$ for half filling and at different values of g is illustrated in Fig. 3. It should be noted that for $n=1$ the above equation reduces to $q=4g/(1+g)^2$, which is the result of Gutzwiller's approximation (GA). This, however, does not imply that, for this particular value of filling, the kinetic energy coincides with that of GA, since g has to be determined by minimizing the total energy, and the equations for the potential energy are different in the two cases.

By combining Eq. (3.32) with the result for the momentum distribution function, one may calculate $E_0(g)$ in one dimension for the paramagnetic ground state. Minimization with respect to g yields the energy for given values of t, U, n. For $n=1$, the comparison with the result of Gutzwiller's approximate treatment and the exact result of Lieb and Wu (1968) shows that the GVW, when exactly handled, gives an energy that is intermediate between the other two. This is illustrated in Fig. 4. In particular, specializing to the case $n=1$ and $U/t\to\infty$, with only nearest-neighbor hopping, one finds $\bar{\epsilon}_0=-4t/\pi$, and

$$E/N = -(4/\pi)^2(t^2/U)(\ln\bar{U})^{-1} , \tag{3.34}$$

where $\bar{U}=U/|\bar{\epsilon}_0|$. We note, with reference to the numerical results of Kaplan *et al.* discussed earlier, that the energy is certainly proportional to t^2/U, but the proportionality factor goes logarithmically to zero with U/t. Thus, for the half-filled-band case, the GVW gives a result that is qualitatively different from the exact result. From Eq. (3.33) it is clear that a discontinuity in the momentum distribution remains at any finite U, whereas the exact solution of the Hubbard model of Lieb and Wu (1968) gives an insulating system for any nonzero U (see also Ferraz *et al.*, 1978). It would seem from these considerations that the GVW is not a particularly good ansatz for the ground state of the Hubbard model. However, we have already seen from the results of Kaplan *et al.* that it performs much better in the calculation of spin-spin correlations than for the energy.

Using techniques similar to those employed in the energy calculations, Gebhard and Vollhardt (1987) have calculated, for the paramagnetic ground state, a number of correlation functions,

$$C_j^{XY} = N^{-1}\sum_i \langle X_i Y_{i+j}\rangle - \langle X\rangle\langle Y\rangle , \tag{3.35}$$

where $X_i, Y_i = S_i^z, n_i, D_i, H_i$. Here $n_i = n_{i\uparrow}+n_{i\downarrow}$, and $H_i=(1-n_{i\uparrow})(1-n_{i\downarrow})$ is the number operator for the holes. In addition, $X=N^{-1}\sum_i X_i$, and the Fourier transforms of the functions defined in Eq. (3.35) are sim-

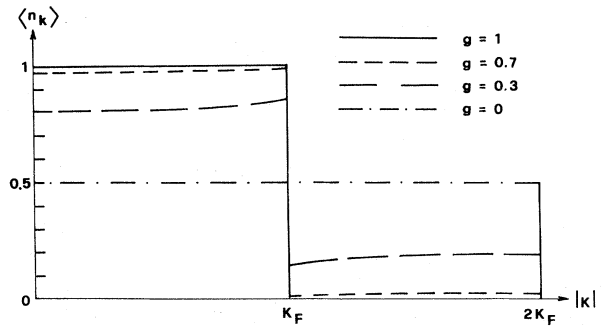

FIG. 3. Momentum distribution $\langle n_k\rangle$ for the one-dimensional Hubbard model. The results obtained by using the Gutzwiller variational wave function are shown for several values of the correlation parameter g in the case of a half-filled band ($n_\uparrow = n_\downarrow = \frac{1}{2}$). From Metzner and Vollhardt (1987).

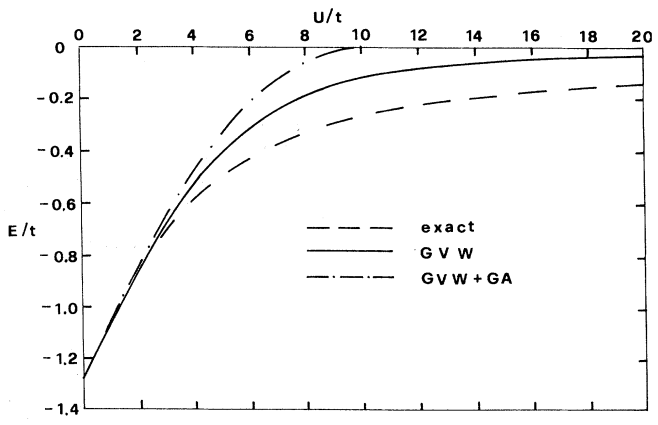

FIG. 4. Ground-state energy E for the one-dimensional Hubbard model with $n_\uparrow = n_\downarrow = \frac{1}{2}$ as a function of U. The results for E, as calculated with the Gutzwiller variational wave function (GVW), are compared with the result of the Gutzwiller approximation (GA). From Metzner and Vollhardt (1987).

ply denoted by $C^{XY}(q)$. The results for the spin-spin correlation function $q_l \equiv C_l^{SS}$ obtained by Gebhardt and Vollhardt fully confirm the numerical calculations of q_1 by Kaplan *et al.* However, with the analytical solution it is possible to establish that there is, in fact, a difference of 0.2% between the exact and the GVW results in the atomic limit, and that such a difference is not due to numerical uncertainties. In addition, the features of the exact q_l found in numerical investigation (Betsuyaku and Yokota, 1986; Kaplan *et al.*, 1987) on the Heisenberg antiferromagnetic chain are reasonably reproduced, though the agreement worsens at larger distances, as already suggested by Kaplan *et al.* (1982). The comparison between the GVW result and the exact result for the hole-hole correlation function $C^{HH}(q)$ in the atomic limit also shows an overall agreement, which tends to improve as the number of holes tends to zero. Finally, we notice that Gebhardt and Vollhardt also comment on the correlations between holes and doubly occupied sites. Their conclusion is that these kinds of correlations are not described particularly well by the GVW and that this might well be the reason for the logarithmic singularity found in the energy for $g \to 0$.

2. Numerical results

Recently, a number of numerical investigations on the Hubbard model with the GVW were conducted with the help of the Monte Carlo method. One should distinguish between two kinds of investigations. In one case the original Gutzwiller program is implemented; i.e., ground-state properties of the Hubbard Hamiltonian are variationally calculated with the wave function of Eq. (3.8), for arbitrary n, t, U and dimensionality. In the other case, following the observation of Kaplan *et al.* (1982) that the GVW for $g = 0$ gives an accurate description of spin correlation in the Heisenberg antiferromagnetic chain, one works on the effective Hamiltonian to which the Hubbard one reduces in the limit $U \to \infty$, thus restricting one to the strong-coupling situation.

Yokoyama and Shiba (1987a) have systematically studied the Hubbard model, following the first of the above-mentioned approaches. Thus they have performed calculations in one, two, and three dimensions over the full range of coupling U/t and for both half-filled and non-half-filled bands. Here we shall not enter into the technical details of their variational Monte Carlo technique, with which they performed calculations with up to 216 sites ($6 \times 6 \times 6$ in three dimensions). We shall merely give a brief review of their main results.

In one dimension and for $n = 1$, they have calculated E_{kin}/t and $d = E_{\text{pot}}/U$ as functions of g between 0 and 1. For a given value of U, one can then construct from such functions the total energy as a function of g and find its minimum by inspection. They have also calculated the momentum distribution. We merely note that in this case the exact solution is available and that according to Metzner and Vollhardt (1987) the agreement with their analytic results is excellent. In the limit in which $U \to \infty$, however, they have not been able to isolate the logarithmic correction to the quadratic dependence t^2/U of the energy, but it would have been surprising otherwise. Similar calculations were performed for the test case $n = 0.84$, taken as representative of a band less than half filled. The results for the energy are in fair agreement with the exact result, even if they observe that improvements upon the GVW are called for if one wishes to obtain better agreement. The need to take into account intersite correlation is also mentioned, a point that has already been stressed by Stollhoff and Fulde (1977), as we discussed at some length earlier.

In two dimensions only the case $n = 1$ on a square lattice was considered. They found, for the total energy, that the variational results and those of the Gutzwiller approximation are much closer than they were in one dimension, as can be seen by comparing the 2D case reported in Fig. 5 with the 1D case in Fig. 4. This is in accord with the expectation that the GA should become more accurate in higher dimensions. However, comparison with the Hartree-Fock antiferromagnetic energy shows that the discrepancies with this are sizable for large U, whereas they were much smaller in one dimension.

The calculations in three dimensions were performed for a cubic lattice and again for a half-filled band. The results for the total energy as a function of the interaction strength U/t are similar to those found in two dimensions. Furthermore, in going from two to three dimensions, changes qualitatively similar to those observed in going from one to two dimensions are apparent. Thus the agreement between variational and approximate treatments, i.e., with the GA, improve further, while for large U the discrepancy with the antiferromagnetic Hartree-Fock energy, which is lower, remains sizable.

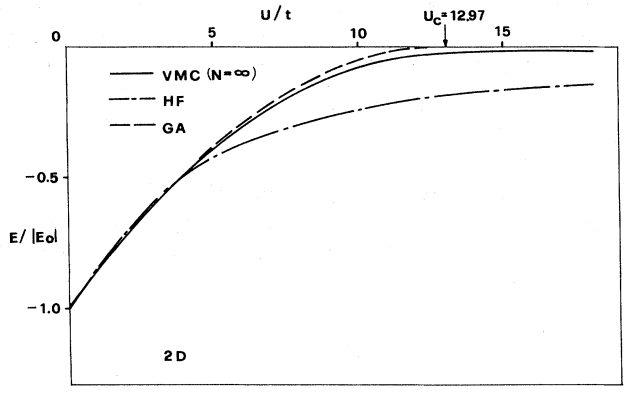

FIG. 5. Normalized ground-state energy for the two-dimensional Hubbard model as a function of U: VMC, variational Monte Carlo with the Gutzwiller variational wave function (extrapolated at an infinite number of sites, $N = \infty$); HF, antiferromagnetic Hartree-Fock; GA, Gutzwiller approximation. The half-filled-band case ($n_\uparrow = n_\downarrow = \frac{1}{2}$) is shown. From Yokoyama and Shiba (1987a).

This suggests that, in two and three dimensions, one should perform the variational calculations using a GVW based on the Hartree-Fock ground state of the antiferromagnetic system, rather than on that of the paramagnetic one.

To introduce the second of the approaches mentioned above, we shall briefly summarize the derivation of the effective Hamiltonian which can be obtained from the Hubbard one for strong couplings U/t. We shall follow the very straightforward method given by Gros *et al.* (1987a), but reference should also be made to Castellani *et al.* (1979) and to Hirsch (1985). One can start from the Hubbard Hamiltonian given in Eq. (3.10) and rearrange the kinetic energy T, specializing to the case of nearest-neighbor hopping, to read

$$H = T_h + T_d + T_{\rm mix} + V \ , \tag{3.36}$$

with

$$T_h = -t \sum_{\langle ij \rangle, \sigma} (1-n_{i,-\sigma}) a_{i\sigma}^{\dagger} a_{j\sigma} (1-n_{j,-\sigma}) \ , \tag{3.37}$$

$$T_d = -t \sum_{\langle ij \rangle, \sigma} n_{i,-\sigma} a_{i\sigma}^{\dagger} a_{j\sigma} n_{j,-\sigma} \ , \tag{3.38}$$

$$T_{\rm mix} = -t \sum_{\langle ij \rangle, \sigma} n_{i,-\sigma} a_{i\sigma}^{\dagger} a_{j\sigma} (1-n_{j,-\sigma}) - t \sum_{\langle ij \rangle, \sigma} (1-n_{i,-\sigma}) a_{i\sigma}^{\dagger} a_{j\sigma} n_{j,-\sigma} \ , \tag{3.39}$$

where T_h and T_d are the kinetic energies describing the propagation of holes and doubly occupied sites, respectively, in their Hubbard bands, and $T_{\rm mix}$ is clearly a mixing term that couples such bands. V is, of course, the usual on-site repulsion energy, $V = U \sum_i n_{i\uparrow} n_{i\downarrow}$. The next step is to apply to the Hamiltonian a suitable unitary transformation,

$$H_{\rm eff} = e^{iS} H e^{-iS} = H + i[S,H] + \cdots \ , \tag{3.40}$$

such that, in lowest order in t/U, $T_{\rm mix}$ vanishes on the right-hand side of Eq. (3.40). This can be accomplished by choosing S such that $i[S, T_h + T_d + V] = -T_{\rm mix}$, i.e.,

$$S = \sum_{n,m} |n\rangle \frac{\langle n | T_{\rm mix} | m \rangle}{i(\epsilon_n - \epsilon_m)} \langle m| \ , \tag{3.41}$$

with $|n\rangle$ and $|m\rangle$ being eigenstates of $T_h + T_d + V$. Even if these eigenstates are not known in the general case, for very large U it must be $\epsilon_n - \epsilon_m = \pm U + O(t)$. Thus one gets

$$S = -\frac{it}{U} \sum_{\langle ij \rangle, \sigma} n_{i,-\sigma} a_{i\sigma}^{\dagger} a_{j\sigma} (1-n_{j,-\sigma}) + \frac{it}{U} \sum_{\langle ij \rangle, \sigma} (1-n_{i,-\sigma}) a_{i\sigma}^{\dagger} a_{j\sigma} n_{j,-\sigma} \ . \tag{3.42}$$

If, as is the case here, one is interested in taking matrix elements of $H_{\rm eff}$ between states with no doubly occupied sites, such as the infinite-U Gutzwiller wave function of Eq. (3.24), it can be easily shown that $H_{\rm eff}$ can be written as

$$H_{\rm eff} = T_h + i[S, T_{\rm mix}] + SVS = T_h + \frac{2t^2}{U} \sum_i \sum_{\tau,\tau'} [(a_{i+\tau}^{\dagger} \mathbf{s} a_{i+\tau'}) \cdot (a_i^{\dagger} \mathbf{s} a_i) - \tfrac{1}{4} (a_{i+\tau}^{\dagger} a_{i+\tau'}) \cdot (a_i^{\dagger} a_i)] \ . \tag{3.43}$$

Above, $a_i \mathbf{s} a_j \equiv \sum_{\sigma\sigma'} a_{i\sigma}^{\dagger} (\mathbf{s})_{\sigma\sigma'} a_{j\sigma'}$ and $a_i a_j \equiv \sum_{\sigma} a_{i\sigma}^{\dagger} a_{j\sigma}$, with the vector $\mathbf{s}$ being the spin operator, and the indices τ and τ' running over the first neighbors of i. We should note two things. In Eq. (3.43) we have also considered the term SVS, which would appear as of higher order in S. But the expansion parameter is t/U, and such a term turns out to be of the same order of $i[S, T_{\rm mix}]$. In addition, if three-site terms (i.e., $\tau \neq \tau'$) can be neglected, then Eq. (3.43) simplifies to

$$H_{\rm eff} = T_h + \frac{2t^2}{U} \sum_{\langle ij \rangle} (\mathbf{s}_i \cdot \mathbf{s}_j - \tfrac{1}{4} n_i n_j) \ , \tag{3.44}$$

with $n_i = n_{i\uparrow} + n_{i\downarrow}$ being the site number operator. This is exactly true for the half-filled-band case, for which one also has $n_i = 1$. However, for $n \neq 1$, three-site contributions may become important, as has recently been discussed by Yokoyama and Shiba (1987b). It should be noted that calculating averages of $H_{\rm eff}$ on $|\Phi_\infty\rangle$ is equivalent to calculating averages of H on a modified wave function $|\tilde{\Phi}_\infty\rangle = (1 - iS)|\Phi_\infty\rangle$, that is, $\langle |\Phi_\infty| H_{\rm eff} |\Phi_\infty\rangle = \langle |\tilde{\Phi}_\infty| H |\tilde{\Phi}_\infty\rangle$, provided terms of order t^2/U^2 have been neglected. In particular, the number of doubly occupied sites is nonzero on this wave function, or, more precisely, of order t^2/U^2. For the half-filled band, if one puts $H_{\rm eff} = T_h + V_{\rm corr}$, then

$$D = \langle \tilde{\Phi}_\infty | \frac{1}{U} V | \tilde{\Phi}_\infty \rangle = -\frac{1}{2U} \langle \Phi_\infty | V_{\rm corr} | \Phi_\infty \rangle \ . \tag{3.45}$$

Before turning to the numerical results that have recently been obtained by employing the strong-coupling Hamiltonian of Eq. (3.43) or (3.44), we should like to stress one point. As observed first by Kaplan *et al.* (1982), $|\Phi_\infty\rangle$, while giving a good description of the spin-spin correlations, yields poor results, if used to calculate the energy directly from the Hubbard Hamiltonian. One should have clearly in mind therefore that $|\Phi_\infty\rangle$ is a good ground state for $H_{\rm eff}$, but not for H. Thus the combined use of $H_{\rm eff}$ and $|\Phi_\infty\rangle$ is equivalent, as we have already noted, to working with the Hubbard Hamiltonian, but using an improved Gutzwiller-like wave function.

Using the approach mentioned above, i.e., working in terms of $H_{\rm eff}$ and $|\Phi_\infty\rangle$, Gros *et al.* (1987a) have conducted an extensive Monte Carlo study of the Hubbard model for strong coupling. They restrict their investigation to one dimension to obtain good numerical accuracy, even if their interest is, of course, in the three-dimensional situation. On the other hand, they consider variable band filling, magnetization, and degeneracy N_f of the local state. Their results for the spin-spin correlation function q_1 at half-filling have established, before the exact solution with the GVW appeared (Gebhard and

Vollhardt, 1987), that the small difference between the exact result for this quantity and that obtained from the infinite-U Gutzwiller wave function is beyond the numerical uncertainty of the Monte Carlo calculation. The investigation of the kinetic energy as a function of the filling, on the other hand, shows good agreement with the exact result of both Monte Carlo and GA results. Gros, Joynt, and Rice also discuss the fact that for large U the hole-hole correlation function can be put into correspondence with that of a system of spinless noninteracting fermions. This allows for an assessment of the quality of their results. They find fair agreement, even if some qualitative features of the exact result, related to the presence of a sharp Fermi surface, are missing. Moreover, an enhancement with respect to the exact result of correlations at short distances is found. Regarding the total energy, for large U and values of the filling very close to 1, the accuracy of the Monte Carlo result is dominated by the kinetic-energy contribution, with an accuracy of about 6%. In fact, the potential energy, being determined by q_1, has a much better accuracy, i.e., 0.2%. Finally, they find that when excited-state Gutzwiller wave functions are considered, the accuracy of GA is much reduced. For the cases in which direct comparison with the analytical results of Metzner and Vollhardt (1987) and Gebhard and Vollhardt (1987) was possible, excellent agreement was found.

One of the reasons for the revived interest in the Hubbard Hamiltonian is its possible relevance in the understanding of the mechanism underlying high-temperature superconductivity, as suggested by Anderson (1987). In particular, investigations in the strong correlation regime are called for. The importance of the scheme, briefly outlined above, for dealing with the large coupling situation is then apparent. An investigation in this direction was made recently by Yokoyama and Shima (1987b), within the effective Hamiltonian approach. They used the effective Hamiltonian of Eq. (3.39) and considered both a paramagnetic and an antiferromagnetic ground state. This can be done by simply changing the type of uncorrelated wave function $|\Phi_0\rangle$, from which the Gutzwiller wave function of Eq. (3.24) is built. One and two dimensions were considered. The purpose of the study was to characterize the competition between the two types of ground states. Before briefly summarizing their findings, it should be mentioned that they have also shown that the simple infinite-U Gutzwiller wave function constitutes one of the many possible realizations of Anderson's resonating valence-bond state or singlet state. In one dimension, they find that for both half-filled and non-half-filled bands, the singlet state is stable against the Néel (antiferromagnetic) state. The situation is quite different in two dimensions. For the half-filled case the singlet state is found to be unstable against the Néel state. Whereas the results for the energy and magnetization are in reasonable accord with estimates obtained with different approaches, they question whether the same situation would be found if next-nearest hopping were to be included. Moving from the half-filled band ($n=1$), at very large U, the ferromagnetic state becomes favorable in energy. However, by decreasing n at some point ($n \cong 0.61$) the singlet state takes over again. On the other hand, if U is decreased, the Néel state appears to again decrease in energy. From these results they draw a qualitative phase diagram as shown in Fig. 6. This should be considered meaningful only in the small t/U region, where the effective Hamiltonian approach is appropriate.

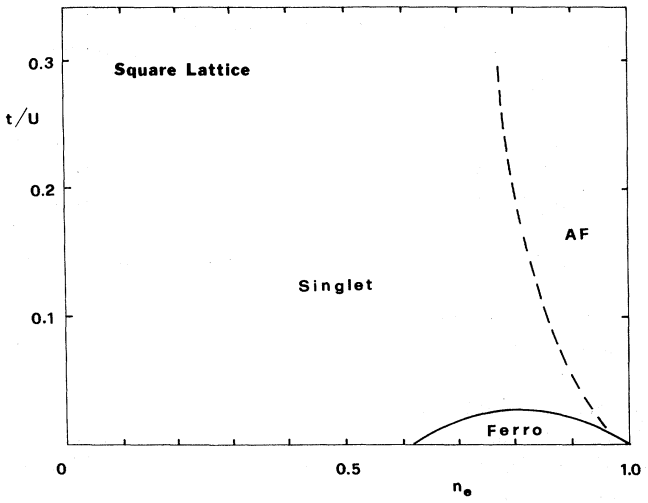

FIG. 6. Phase diagram of the two-dimensional square-lattice Hubbard model, as inferred from variational Monte Carlo using a Gutzwiller-type wave function (Yokoyama and Shiba, 1987b). Here $n_e = n_\uparrow + n_\downarrow$ is the band filling.

Finally, we should mention here the work of Gros, Joynt, and Rice (1987b). Using the effective Hamiltonian approach, they investigate the stability of generalized Gutzwiller wave functions against Cooper pairing, in the large-U limit and in two dimensions. This is done by evaluating the binding energy of two holes in the variational wave function. As they note, no real attempt was made to optimize their wave function. They find that the paramagnetic or singlet state is stable against s-wave pairing but unstable against d-wave pairing. On the other hand, the antiferromagnetic state is stable against both kinds of pairings. They discuss a possible pairing mechanism and the relevance of their results for high-T_c superconductors.

E. Resonating valence-bond states

In the foregoing we have seen how the Hubbard Hamiltonian—for large values of the coupling U—can be transformed into an antiferromagnetic Heisenberg Hamiltonian by means of a suitable unitary transformation. In this connection and also in relation to the high-T_c superconductivity, it seems appropriate here to briefly review the mathematical formulation due to Anderson (1973) of the concept of the resonating valence-bond (RVB) states first put forward by Pauling (1949).

In discussing the ground-state properties of the triangular two-dimensional Heisenberg antiferromagnet for $S=\frac{1}{2}$, Anderson (1973; see, also, Fazekas and Anderson, 1974) proposed that at least for this system, and perhaps also in other cases, the ground state might be the analog of the precise singlet in the Bethe (1931) solution of the linear antiferromagnetic chain. In fact, the zero-order energy of a state consisting purely of nearest-neighbor singlet pairs is more nearly realistic than that of the Néel state.

For electrons on a lattice, one can think of a singlet bond or pair as the state formed when two electrons with opposite spin are localized on two distinct sites. A resonating valence-bond state is a coherent superposition of such singlet bonds; its energy is further lowered as a result of the matrix elements connecting the different valence-bond configurations.

Heuristically, valence bonds can be viewed as real-space Cooper pairs that repel one another, a joint effect of the Pauli principle and the Coulomb interaction. When there is one electron per site, charge fluctuations are suppressed, leading to an insulating state. However, as one moves away from half filling, current can flow; the system becomes superconducting as the valence bonds Bose condense.

Anderson (1987), while stressing the difficulty of making quantitative calculations with RVB states, in fact gives a suggestive representation of them by exploiting the Gutzwiller-type projection technique.

Clearly, a delocalized or mobile valence bond can be written as

$$b_\tau^\dagger|\Phi_0\rangle=\frac{1}{\sqrt{N}}\left[\sum_i a_{i\uparrow}^\dagger a_{i+\tau\downarrow}^\dagger\right]|0\rangle$$
$$=\frac{1}{\sqrt{N}}\left[\sum_k a_{k\uparrow}^\dagger a_{-k\downarrow}^\dagger \exp i(k\cdot\tau)\right]|0\rangle\ , \tag{3.46}$$

where $b_\tau^\dagger$ is the creation operator for a valence-bond state with lattice vector τ; $a_{i\sigma}^\dagger$, the single-electron creation operator; and N, the total number of sites. A distribution of bond lengths can be obtained by summing $b_\tau^\dagger$ over τ with appropriate weights. One then gets a new creation operator,

$$b^\dagger=\sum_k c_k a_{k\uparrow}^\dagger a_{-k\downarrow}^\dagger\ , \tag{3.47}$$

with the restriction

$$\sum_k c_k=0\ , \tag{3.48}$$

if double occupancy is to be avoided.

Anderson proceeds by (a) Bose condensating such mobile valence bonds,

$$|\Phi\rangle=(b^\dagger)^{N/2}|0\rangle\ , \tag{3.49}$$

and by (b) projecting out the double occupancy—which would otherwise be present—with an infinite-U Gutzwiller projection operator $P_d=\prod_i(1-n_{i\uparrow}n_{i\downarrow})$,

$$|\Phi_{\rm RVB}\rangle=P_d(b^\dagger)^{N/2}|0\rangle\ . \tag{3.50}$$

One can then show that the RVB state written above can be obtained with simple manipulations from a standard BCS state by projecting on the state with N particles and projecting out, at the same time, the double occupancy:

$$|\Phi_{\rm RVB}\rangle=P_{N/2}P_d\left[\frac{1}{\sqrt{1+c_k}}+\frac{c_k}{\sqrt{1+c_k}}a_{k\uparrow}^\dagger a_{-k\downarrow}^\dagger\right]|0\rangle\ . \tag{3.51}$$

Baskaran *et al.* (1987) have subsequently shown that by treating the large-U Hamiltonian of Eq. (3.44) with a mean-field (Hartree-Fock) approximation, one obtains precisely a BCS-type Hamiltonian which—for half filling—yields the RVB state heuristically introduced above. In fact, one also finds that $\sum_k c_k=0, |c_k|=1$ and the c_k change sign across what they call a *pseudo-Fermi* surface. We shall not deal here with the nature of excitations from such a RVB state, referring the reader instead to the original papers.

IV. QUANTUM MONTE CARLO CALCULATION OF CORRELATION ENERGY

Until quite recently, two systematic methods have provided the main routes to the calculation of correlation energies for many-electron systems at zero temperature, namely, configuration interaction (CI) and many-body perturbation theory. Relatively recent overviews of these two approaches are available [see, e.g., Shavitt *et al.* (1977) and Wilson (1981)], and therefore we shall not go over that ground in the present article. In the last ten years, however, progress in the calculation of electronic correlation has also been made by using a completely different approach, the so-called quantum Monte Carlo (QMC) method.

The goal of QMC [see, e.g., Ceperley (1981), Reynolds *et al.* (1982), Ceperley and Alder (1984), and Kalos (1984)] is to obtain the exact ground-state wave function of a many-body system by numerically solving the Schrödinger equation in one of its equivalent forms. In practice, this is achieved by means of iterative algorithms, which propagate the wave function from a suitable starting guess to the exact ground-state value. Thus, in the diffusion Monte Carlo (DMC) method, one is concerned directly with the evolution in imaginary time of the wave function, which corresponds to a diffusion process in configuration space. In the Green's-function Monte Carlo (GFMC) technique, on the other hand, a time-integrated form of the Green's function or resolvent is used to propagate the wave function. In fact, in either case the sampling of an appropriate Green's function is required, and this is accomplished by means of suitable random-walk algorithms.

Another implementation of the QMC (Blankenbecler *et al.*, 1981; Scalapino and Sugar, 1981; Koonin *et al.*, 1982) emphasizes the role of the imaginary-time propaga-

tor $e^{-\beta H}$ more directly. For long times β (small temperatures $T=1/\beta$), the imaginary-time propagator is dominated by the ground-state energy E_0. Thus E_0 can be suitably extracted from the knowledge of the partition function $Z=\mathrm{Tr}e^{-\beta H}$ or, equally well, from that of the expectation value of the imaginary-time propagator on a state which is not orthogonal to the ground state. In either case, the key simplification in the calculations comes from the mapping of the problem of interacting particles onto that of independent particles. This is accomplished at the expense of introducing *auxiliary* external fields (Koonin *et al.*, 1982; Hirsch, 1983; Sugiyama and Koonin, 1986) having their own probability density.

In the following, we first review the main features of the QMC method for a many-body system in the DMC and GFMC implementations, discussing also the complications that arise from antisymmetry when dealing with systems of fermions, which is the case of interest here. Some applications of the QMC method—to the study of the homogeneous electron assembly and small molecules—are then briefly summarized. Finally, we give the basic ideas underlying the auxiliary external field technique and review some of the recent results on the two-dimensional Hubbard model.

A. Diffusion Monte Carlo method

The Schrödinger equation in imaginary time for an assembly of N identical particles of mass m interacting with a potential $V(\mathbf{R})$ reads

$$-\frac{\partial\phi(\mathbf{R},t)}{\partial t}=(H-E_T)\phi(\mathbf{R},t)$$
$$=[-D\nabla^2+V(\mathbf{R})-E_T]\phi(\mathbf{R},t)\ , \qquad (4.1)$$

where $D=\hbar/2m$, $\mathbf{R}$ is the $3N$-dimensional vector specifying the coordinates of the particles, t is the imaginary time in units of $\hbar$, and the constant E_T represents a suitable shift of the zero of energy. The (imaginary) time evolution of an arbitrary *trial* wave function is easily obtained from its expansion in terms of the eigenfunctions $\phi_i(\mathbf{R})$ of the Hamiltonian H as

$$\phi(\mathbf{R},t)=\sum_i N_i\exp[-(E_i-E_T)t]\phi_i(\mathbf{R})\ . \qquad (4.2)$$

Here, E_i is the energy eigenvalue corresponding to $\phi_i(\mathbf{R})$, and the coefficients N_i are fixed by the initial conditions, i.e., by the chosen trial wave function. Clearly, for long times one finds

$$\phi(\mathbf{R},t)=N_0\exp[-(E_0-E_T)t]\phi_0(\mathbf{R})\ , \qquad (4.3)$$

provided $N_0\neq 0$. Moreover, if E_T is adjusted to be the true ground-state energy E_0, asymptotically one obtains a steady-state solution, corresponding to the ground-state wave function ϕ_0. Thus the problem of determining the ground-state eigenfunction of the Hamiltonian H is equivalent to that of solving Eq. (4.1) with the appropriate boundary conditions.

It is not difficult to recognize in Eq. (4.1) two equations that are well known in physics, though combined together. In fact, if only the term with the Laplacian were present on the right-hand side of Eq. (4.1), one would have a diffusion equation, such as the equation describing Brownian motion (see, for instance, van Kampen, 1981). On the other hand, by retaining only the term $[V(\mathbf{R})-E_T]\phi(\mathbf{R},t)$, one would obtain a rate equation, that is, an equation describing branching processes such as radioactive decay or birth and death processes in a population.

A convenient manner of *simulating* Eq. (4.1) is as follows. Let $\psi(\mathbf{R})$ be the wave function at $t=0$. One can generate an ensemble of systems (points in the $3N$-dimensional space representing electronic configuration) distributed with density $\psi_T(\mathbf{R})$. Hence the time evolution of the wave function will correspond to the motion in configuration space of such systems or *walkers,* as determined by Eq. (4.1). In particular, the Laplacian and energy terms in Eq. (4.1) will cause, respectively, random diffusion and branching (deletion or duplication) of the walkers describing the wave function. This schematization of the Schrödinger equation is particularly appealing from the practical point of view. However, a density is non-negative. Thus the same should hold for the wave function. This would seem to limit the applicability of such a scheme to the ground state of a bosonic system. For the sake of simplicity, we shall accept this restriction for a while and deal with the complications associated with Fermi statistics later.

Solving the Schrödinger equation in its form (4.1) by random-walk processes with branching is not particularly efficient. In fact, the branching term can become very large whenever the interaction potential $V(\mathbf{R})$ does so, causing large fluctuations in the number of walkers. This slows down the convergence toward the ground state. A more efficient computational scheme is obtained by introducing the so-called *importance sampling.* This amounts to considering the evolution equation for the probability distribution $f(\mathbf{R},t)=\phi(\mathbf{R},t)\psi_T(\mathbf{R})$, rather than directly for the wave function ϕ. By using Eq. (4.1) and the definition of $f(\mathbf{R},t)$, one obtains with a little algebra

$$-\frac{\partial f(\mathbf{R},t)}{\partial t}=-D\nabla^2 f+[E_L(\mathbf{R})-E_T]f+D\nabla[fF_Q(\mathbf{R})]\ . \qquad (4.4)$$

Above, $E_L(\mathbf{R})\equiv H\psi_T/\psi_T$ defines the *local energy* associated with the trial wave function, and

$$F_Q(\mathbf{R})\equiv\nabla\ln|\psi_T(\mathbf{R})|^2=2\nabla\psi_T(\mathbf{R})/\psi_T(\mathbf{R}) \qquad (4.5)$$

is the *quantum trial force,* which drifts the walkers away from regions where $\psi(\mathbf{R})$ is small. Obviously, when dealing with Eq. (4.4), the walkers are to be drawn from the probability distribution f. With a judicious choice of ψ_T, one can make $E_L(\mathbf{R})$ a smooth function close to E_T throughout the configuration space and thus reduce branching. In this respect it is essential that $\psi_T(\mathbf{R})$

reproduce the correct cusp behavior as any two particles approach each other, so as to exactly cancel the infinities originating from $V(\mathbf{R})$. That $F_Q(\mathbf{R})$ is a force acting on the walkers becomes clear by comparing Eq. (4.4) with the Fokker-Planck (FP) equation (see, e.g., van Kampen, 1981). It turns out, with the rate term neglected, that the term containing F_Q has to be identified with the so-called *drift term* of the FP equation, and consequently F_Q must be identified with the external force acting on the walkers. We stress again that an important feature of this force is to drift the walkers away from regions of low probability. In fact, from its definition it is apparent that the force becomes highly repulsive in regions where the trial wave function becomes small, diverging where the latter vanishes. Thus the trial wave function determines the probability with which different regions of configuration space are sampled. Therefore it is important that ψ_T be a good approximation to ϕ_0 in order to keep the walkers mainly in regions of configuration space which are really significant in the statistical averages. We finally observe that the asymptotic solution of Eq. (4.4) is

$$f(\mathbf{R},T)=\psi_T(\mathbf{R})\phi_0(\mathbf{R})\exp[-(E_0-E_T)t] , \tag{4.6}$$

which becomes a steady-state solution when E_T is adjusted to E_0.

The differential equation (4.4) for the probability distribution $f(\mathbf{R},t)$ can be recast in integral form as

$$f(\mathbf{R},t+t')=\int d\mathbf{R}' f(\mathbf{R}',t')K(\mathbf{R}',\mathbf{R},t) , \tag{4.7}$$

where the Green's function $K(\mathbf{R}',\mathbf{R},t)$ is a solution of Eq. (4.4) with the boundary condition $K(\mathbf{R}',\mathbf{R},0)=\delta(\mathbf{R}-\mathbf{R}')$ and is simply related to the Green's function $G(\mathbf{R}',\mathbf{R},t)$ for Eq. (4.1), $K(\mathbf{R}',\mathbf{R},t)=\psi_T(\mathbf{R}')G(\mathbf{R}',\mathbf{R},t)\psi_T^{-1}(\mathbf{R})$. The advantage of the above equation is that for short times t it is possible to write approximate simple expressions for $K(\mathbf{R}',\mathbf{R},t)$ (Moskowitz *et al.*, 1982b; Reynolds *et al.*, 1982). The time evolution of $f(\mathbf{R},t)$ for finite t can then be obtained by successive iterations of Eq. (4.7), starting from the initial distribution $f(\mathbf{R},0)$ and using a small time step. In each time iteration, advantage can be taken of the positivity of K for short times so as to interpret it as a transition density. A suitable modified random-walk algorithm can then be devised, which allows the integration of Eq. (4.7) during a small time interval. The essential steps of such an algorithm are as follows. The walkers representing the initial distribution are allowed to diffuse randomly and drift under the action of the quantum force F_Q. After the new positions have been reached, each walker is deleted or placed in the *new generation* in an appropriate number of copies, depending on the size of the local energy at the old and at the new position relative to the reference energy E_T. Finally, the number of walkers in the new generation is renormalized to the initial population. The interested reader may find a detailed description of such a random-walk algorithm in Reynolds *et al.* (1982).

Once the long-time probability distribution has been obtained and made stationary by a suitable shift of the constant E_T, one can estimate equilibrium quantities. For the ground-state energy E_0, in particular, by using the fact that H is Hermitian, one finds

$$E_0=\frac{\int \psi_T H\phi_0}{\int \psi_T\phi_0}=\frac{\int E_L f}{\int f}=\frac{\sum_i E_L(\mathbf{R}_i)}{\sum_i} . \tag{4.8}$$

The sum on the right-hand side of the above equation runs over the positions of all the walkers representing the equilibrium probability distribution.

It should be stressed that the short-time approximation to the Green's function introduces a systematic error in the computations. However, this error should decrease with a decrease in the time step. Moreover, in the calculation by Reynolds *et al.* (1982), an acceptance/rejection step was used which, within the calculational scheme outlined above, should correct for the approximate nature of G.

B. Green's-function Monte Carlo technique

We have seen that in the diffusion Monte Carlo method one starts from the Schrödinger equation in imaginary time in order to construct an integral equation which can then be solved iteratively. Such an equation contains a time-dependent Green's function. In the Green's-function Monte Carlo technique, one proceeds in a similar fashion, starting, however, from the Schrödinger eigenvalue equation. The resulting integral equation, as we shall see, differs from Eq. (4.7) mainly through the absence of time. In fact, it could be directly obtained from Eq. (4.7) by a straightforward time integration (Ceperley and Alder, 1984). Here, however, we choose to follow another route (Ceperley and Kalos, 1979; Kalos, 1984) which in the present context is somewhat more instructive.

The Schrödinger eigenvalue equation for an N-body system, described by the Hamiltonian H introduced in Eq. (4.1), is

$$H\phi(\mathbf{R})=E\phi(\mathbf{R}) . \tag{4.9}$$

Let us assume that the potential $V(\mathbf{R})$ appearing in H is such that the spectrum of H is bounded from below, E_0 being the lowest eigenvalue, i.e., the ground-state energy. This is a natural assumption for a physical system in the nonrelativistic limit. One can choose a positive constant V_0 such that $E_0+V_0>0$, and rewrite Eq. (4.9) as

$$(H+V_0)\phi(\mathbf{R})=(E+V_0)\phi(\mathbf{R}) . \tag{4.10}$$

The resolvent $G(\mathbf{R},\mathbf{R}')$, i.e., the Green's function for Eq. (4.10), is then defined by

$$(H+V_0)G(\mathbf{R},\mathbf{R}')=\delta(\mathbf{R}-\mathbf{R}') . \tag{4.11}$$

Due to the manner in which V_0 has been chosen, it is

clear that the operator $H+V_0$ is positive definite. This is immediate in the energy representation. The same, of course, holds for the inverse operator $G=1/(H+V_0)$. Actually, a much more strict inequality involving G can be established, namely,

$$G(\mathbf{R},\mathbf{R}')=\langle \mathbf{R}|G|\mathbf{R}'\rangle \geq 0 \quad \text{for all } \mathbf{R},\mathbf{R}' , \tag{4.12}$$

which is of central importance for the calculational scheme that we are about to describe. A brief sketch of how one can prove the inequality (4.12) is given in Appendix B. Here, we merely note for future reference that G is integrable. Therefore, because of the above inequality, it can be regarded as a probability, or more precisely as a transition density.

A space integration of Eq. (4.10), after multiplying by $G(\mathbf{R},\mathbf{R}')$ and utilizing Eq. (4.11), yields the desired integral equation,

$$\phi(\mathbf{R})=(E+V_0)\int d\mathbf{R}'G(\mathbf{R},\mathbf{R}')\phi(\mathbf{R}') . \tag{4.13}$$

In the above equation one has to solve simultaneously for E and $\phi(\mathbf{R})$. However, if one has a trial wave function $\psi_T(\mathbf{R})$ and, consequently, a trial energy E_T, it is tempting to try solving Eq. (4.13) by iteration. One would generate a sequence of wave functions, according to

$$\Phi_n(\mathbf{R})=(E_T+V_0)\int d\mathbf{R}'G(\mathbf{R},\mathbf{R}')\Phi_{n-1}(\mathbf{R}') \tag{4.14}$$

and with $\Phi_0(\mathbf{R})=\psi_T(\mathbf{R})$. In fact, this series converges precisely to the ground-state wave function, and it does so exponentially fast. This can be easily seen by expanding both $G(\mathbf{R},\mathbf{R}')$ and $\Phi_0(\mathbf{R})$ in eigenfunctions of H,

$$G(\mathbf{R},\mathbf{R}')=\sum_i \frac{\phi_i(\mathbf{R})\phi_i(\mathbf{R}')}{E_i+V_0} , \tag{4.15}$$

$$\Phi_0(\mathbf{R})=\sum_i c_i\phi_i(\mathbf{R}) . \tag{4.16}$$

One immediately finds

$$\Phi_n(\mathbf{R})=\sum_i \left[\frac{E_T+V_0}{E_i+V_0}\right]^n c_i\phi_i(\mathbf{R}) . \tag{4.17}$$

So, provided $c_0\neq 0$, one obtains

$$\lim_{n\to\infty}\Phi_0(\mathbf{R})\propto c_0\phi_0(\mathbf{R}) , \tag{4.18}$$

which is the desired result.

As in the case of the diffusion Monte Carlo method, one has cast the problem of finding the ground-state wave function and energy of a given Hamiltonian in integral form, suitable for iterative techniques. For the sake of simplicity, we shall temporarily restrict the discussion to bosonic systems, for which both $G(\mathbf{R},\mathbf{R}')$ and the ground-state wave function are non-negative. If one assumes for a while that $G(\mathbf{R},\mathbf{R}')$ is known, a random-walk algorithm similar to the one described for the diffusion Monte Carlo technique is readily constructed. One can proceed as follows. First, at random, an initial population of walkers is drawn from the probability distribution $\Phi_0(\mathbf{R})$, say, at the positions $\{\mathbf{R}_i\}$. Then, a new set of configurations $\{\mathbf{R}'_j\}$ is generated at random, with each one having a conditional density $\sum_i (E+V_0)G(\mathbf{R}_i,\mathbf{R}'_j)$. This density determines the number of walkers corresponding to each new configuration. Finally, a renormalization of the new walker population to the initial size yields the new generation. The above series of steps corresponds to the first iteration of Eq. (4.14). The successive iterations can be performed in the same manner, by only changing the first step. In the nth iteration, in fact, one has to take as the initial population of walkers the new generation of the previous iteration.

It is clear from Eq. (4.17) that the change in size of the walker population is determined by the trial energy E_T. Depending on whether this is larger or smaller than the true ground-state energy E_0, the population will asymptotically grow or decline. This suggests a way of estimating the ground-state energy (Ceperley and Kalos, 1979). In fact, from the space integration of Eq. (4.17) it follows that asymptotically

$$E_0=E_T+V_0\left[\frac{N_n}{N_{n+1}}-1\right] , \tag{4.19}$$

with N_n the initial walker population in the nth iteration and N_{n+1} the new walker population but before size renormalization. The above energy estimator, known as the *growth* estimator, is unfortunately biased even in the limit in which Φ_n is converging to ϕ_0, as discussed by Ceperley and Kalos (1979). A better energy estimator is the one introduced with Eq. (4.8), when describing the diffusion Monte Carlo method. However, in order to use that estimator one has to work with the density $f(\mathbf{R})=\phi(\mathbf{R})\psi_T(\mathbf{R})$ rather than directly with the wave function. This can be easily arranged by multiplying Eq. (4.13) by $\psi_T(\mathbf{R})$ on either side, so as to obtain the new integral equation

$$f(\mathbf{R})=(E+V_0)\int d\mathbf{R}'K(\mathbf{R},\mathbf{R}')f(\mathbf{R}') , \tag{4.20}$$

where

$$f(\mathbf{R})=\phi(\mathbf{R})\psi_T(\mathbf{R}) \tag{4.21}$$

and

$$K(\mathbf{R},\mathbf{R}')=\psi_T(\mathbf{R})G(\mathbf{R},\mathbf{R}')\psi_T^{-1}(\mathbf{R}') . \tag{4.22}$$

Clearly, Eq. (4.20) can still be simulated by means of the random-walk algorithm already described, with $f(\mathbf{R})$ and $K(\mathbf{R},\mathbf{R}')$ replacing, respectively, $\phi(\mathbf{R})$ and $G(\mathbf{R},\mathbf{R}')$. Within such a calculation scheme, successive iteration of Eq. (4.20) will produce a walker population that will asymptotically tend to be distributed with density $f=\phi_0\psi_T$. Consequently, the *local* energy estimator of Eq. (4.8) will also tend to the exact ground-state energy.

In the foregoing we have assumed knowledge of $G(\mathbf{R},\mathbf{R}')$. In practice, for a system of interacting particles, G is not known and must also be sampled by means

of suitable techniques. This can be achieved by relating the exact Green's function G to some trial or reference Green's function G_T, which is known analytically or is numerically calculable. In the domain Green's-Function method of Kalos *et al.* (1974; see also Ceperley and Kalos, 1979 and Moskowitz and Schmidt, 1986), the trial Green's function is taken to be that appropriate to independent particles in a constant potential, with the motion restricted to a subdomain of the whole space. In another implementation of GFMC due to Ceperley (1983; see also Ceperley and Alder, 1984), a better trial Green's function is introduced, which is much closer to the exact one and is defined over the whole space. In either case, the integral equation relating G_T to G is such that a random-walk algorithm, somehow similar to the one outlined above for the calculation of f, can be used. In fact, a global random-walk algorithm can be devised that combines the iterations of Eq. (4.20) with those needed to correct for the difference between G and G_T. Details as to how this is done in practice are to be found in the references quoted above. Here, we shall simply observe again that, in the approach due to Ceperley and Alder (1984), Eq. (4.20) is obtained as a time average or Laplace transform of Eq. (4.7). In addition, the sampling of the time-integrated Green's function [$K(\mathbf{R},\mathbf{R}')$ in the present notation] is obtained also in practical calculations by summing its time-dependent counterpart. This makes such an approach very similar to the diffusion Monte Carlo method, while removing the truncation error due to the use of a finite time step.

C. Quantum Monte Carlo technique with fermions: Fixed-node approximation and nodal relaxation

Here we shall discuss the modifications that one can make to the calculational schemes described above when the restriction of a non-negative wave function is relaxed. Of course, this is necessary if one is to be able at all to deal with Fermi systems and, in general, with excited states of the many-body Hamiltonian H, introduced in Eq. (4.1).

For the sake of clarity, let us briefly recall the relation between the eigenfunctions of H and those of a many-body system described by H but also obeying Bose or Fermi statistics. For bosons (with zero spin), only those wave functions of H that are symmetric under the exchange of any two particle coordinates are admissible solutions. On the other hand, the ground-state wave function of H is completely symmetric, since the ground-state energy is nondegenerate and H commutes with any particle permutation. So, the ground state of H, which of course is characterized by a non-negative wave function, is also the bosonic ground state. Needless to say, the bosonic excited states will have wave functions with positive and negative regions. For fermions, the symmetry of the wave functions is determined by the chosen spin configuration that we shall denote here by s. In general, for many fermions it will always be true that a certain number of particles, say, M, will have the same spin projection. The admissible wave functions of H will then be only those which are antisymmetric with respect to the permutation of any two particle coordinates, within the group of particles having the same spin projections. This is equivalent to saying that only excited states of H can be considered, since, as we have already observed, its ground-state wave function is completely symmetric. It follows at once that the fermionic wave functions must have positive and negative regions, separated by nodal surfaces in the $3N$-dimensional space of the particle coordinates.

The need for dealing with wave functions $\phi(\mathbf{R})$ that change sign would seem to preclude the use of random-walk algorithms such as those discussed above, in that they require a positive wave function. In fact, if one knew the location of the nodal surfaces and consequently of the connected domains in which they break the whole space, the problem would not be a real one. Since the equations involved in the evolution of the wave function are linear, one could just consider in each domain the evolution of the modulus of ϕ. However, such nodal surfaces are not known in more than one dimension, and the problem remains. A simple way of remedying it is to take as nodal surfaces those of the trial wave function $\psi_T(\mathbf{R})$, assumed to be a good approximation to the exact wave function at least in the location of such surfaces. This approximation corresponds to a solution of the Schrödinger equation within a restricted class of functions, and so it should have a variational character. As such it should yield energies that are upper bounds to the exact ones, in the absence of other approximations or sources of error.

A practical way of realizing this so-called fixed-node approximation, within calculations based on random-walk algorithms, is to delete those walkers that, during the calculation, cross a nodal surface of the trial wave function (see, for instance, Reynolds *et al.*, 1982). An alternative and better choice, however, is merely to reject those moves which correspond to such crossings (see the recent discussion on this point by Umrigar *et al.*, 1991). These are simple procedures for enforcing the vanishing of the wave function at the nodal surfaces. In fact, both procedures correspond to solving the Schrödinger equation separately in each domain, the evolution of the walkers in one domain having become independent from that in the other domains. More precisely, if $\{V_\alpha\}$ denotes the domains bounded by the nodal surfaces of ψ_T, one is solving for the ground state of the Hamiltonian H in each domain V_α, according to

$$H\phi_\alpha(\mathbf{R},s)=\varepsilon_\alpha\phi_\alpha(\mathbf{R},s)\ , \tag{4.23}$$

and

$$\phi_\alpha(\mathbf{R},s)\psi_T(\mathbf{R},s)>0,\quad \mathbf{R}\in V_\alpha\ , \tag{4.24}$$

$$\phi_\alpha(\mathbf{R},s)=0,\quad \mathbf{R}\notin V_\alpha\ . \tag{4.25}$$

Above, we have also indicated the spin configuration s.

It should be clear that within the random-walk approach, the asymptotic stationarity of the walker population can only be attained if $E_T=\varepsilon_m$, with ε_m being the minimum among all the ε_α corresponding to volumes V_α which were populated at the beginning of the random walk. Therefore, if the trial energy E_T is suitably adjusted so as to yield stationarity, the asymptotic walker population will be distributed with density

$$f_\infty(\mathbf{R})=f(\mathbf{R},t\to\infty)=c_m\phi_m(\mathbf{R},s)\psi_T(\mathbf{R},s)\ . \quad (4.26)$$

We wish now to make our statement about the variational nature of the fixed-node approximation more precise. First of all, we notice that since H is completely symmetric under the exchange of any two particle coordinates, the symmetry of wave functions is preserved during the evolution, i.e., the random walk. Thus from any one of the ϕ_α, which is defined in a given domain, a wave function with the antisymmetry dictated by the chosen spin configuration can be formally constructed by summing the given ϕ_α over all the permutations P of the electrons, according to

$$\hat{\phi}_\alpha(\mathbf{R},s)=\sum_P(-)^P\hat{\phi}_\alpha(P\mathbf{R},s)\ . \quad (4.27)$$

From the variational principle applied to the Hamiltonian H it follows that the variational energy associated with the above wave function satisfies

$$\frac{\int d\mathbf{R}\hat{\phi}_\alpha^* H\hat{\phi}_\alpha}{\int d\mathbf{R}\hat{\phi}_\alpha^*\hat{\phi}_\alpha}=\varepsilon_\alpha>E_0\ , \quad (4.28)$$

where E_0 is the minimum eigenvalue among those relative to the eigenfunctions of H with the given symmetry, i.e., is the exact energy of the fermionic ground state, for the given spin configuration. On the other hand, from Eq. (4.26) and the Hermiticity of H it also follows that the local energy estimator, which was explicitly given in Eq. (4.8), tends asymptotically to ε_m. This completes the proof that the fixed-node approximation yields a variational upper bound to the exact ground-state energy of a fermionic system.

Before discussing to what extent it is possible to improve on the fixed-node approximation, it is worth noting a detail which may appear technical at this point, but will prove useful in what follows. In applying the above scheme, one is solving the Schrödinger equation by means of random walks separately in each of the domains fixed by the trial antisymmetric function ψ_T. In practice, the sign of ψ_T is needed so as to delete those walkers that change domains, or, better, to reject those moves that imply such crossings. It should be clear to the reader that, with regard to importance sampling, nothing changes if one defines a *guidance* function ψ_G to be positive everywhere and takes as distribution $f=\phi\psi_G$, provided that the sign of ψ_T is still used to locate the nodal surfaces. In fact, the fixed-node approximation, as presented above, corresponds to taking $\psi_G=|\psi_T|$. However, nothing changes in the foregoing discussion if one makes a different choice for ψ_G. We stress that, to yield an efficient sampling, ψ_G should, in any case, be a good approximation to the modulus of the exact ground state. This is equivalent to saying that ψ_G should not differ too much from $|\psi_T|$, since ψ_T was assumed from the start to be a good approximation to the exact ground state.

It was mentioned that the difficulties in applying a random-walk algorithm to the calculation of the Fermionic ground state arise from the fact that the corresponding wave function possesses positive and negative regions and therefore cannot be regarded as a walker's density. However, this difficulty is easily remedied, at least formally. The manner in which this can be done is as follows. One can simply regard positive and negative regions of the trial wave function as determining the positive densities of different objects, the white and black walkers. In fact, an antisymmetric wave function can always be written as the difference between two positive functions. The partitioning in white and black walkers mentioned above corresponds to a particular choice of such functions. It is clear from the linearity of Eqs. (4.1) and (4.14) that one can consider the evolution of each one of these functions separately. At each step of the iteration process yielding the evolution, the difference between the two functions will give an antisymmetric wave function (Kalos, 1984).

The approach outlined above to the problem of Fermi statistics is the essence of the so-called nodal relaxation method (Ceperley and Alder, 1980, 1984; Ceperley, 1981). However, while it seems relatively simple and straightforward, such a method turns out to be unstable when numerically implemented. The reason for this is clear. The two positive functions into which the antisymmetric wave function is divided are no longer antisymmetric. As such, they acquire a projection onto the symmetric Bose ground state, which has a lower energy than the Fermi ground state. As the evolution proceeds, the Bose component of each one of the functions grows exponentially with respect to the antisymmetric component. Thus, in principle, in taking the difference between the two functions, the Bose component should cancel out, leaving the antisymmetric Fermi component. In practice, because of the finite numerical precision, after a sufficient number of iterations the latter component is completely lost, and the difference between the two functions is just noise. This is a manifestation of the so-called *fermion sign problem*. In order to avoid the loss of the fermionic signal, one has to suitably restrict the evolution time. Therefore it is important that the trial wave function be very close to the exact Fermi ground state, since the closer it is the shorter the evolution time can be made. For the above reasons, the estimates of the Fermi ground state based on the nodal relaxation method have also been termed "transient estimates" (Kalos, 1984).

Before closing this necessarily incomplete presentation of the quantum Monte Carlo technique, we intend to give a very brief idea of the way the nodal relaxation method has been practically implemented (see, for instance,

Ceperley and Alder, 1984). To fix ideas, we shall consider the application of the method within the Green's-function formalism with importance sampling. Thus the starting point is Eq. (4.20), which gives the evolution of the distribution $f(\mathbf{R})=\phi(\mathbf{R})\psi_T(\mathbf{R})$. We shall, however, distinguish between a trial wave function, which provides the initial nodal surfaces, and a positive guidance function, to be used in the importance sampling. In this manner one can deal with the evolution of a positive distribution, for which a random-walk algorithm can still be used, and attach to each walker the appropriate sign at the end, in a way which depends on the number of crossings of the walker through the nodal surfaces of ψ_T.

Since the importance sampling is made according to ψ_G, it is useful to introduce a corresponding Green's function,

$$D(\mathbf{R},\mathbf{R}')=\psi_G(\mathbf{R})G(\mathbf{R},\mathbf{R}')\psi_G^{-1}(\mathbf{R}') , \tag{4.29}$$

and an appropriate weight function,

$$W(\mathbf{R})=\psi_T(\mathbf{R})\psi_G^{-1}(\mathbf{R}) . \tag{4.30}$$

The relation between the above Green's function and the one defined in Eq. (4.22) is

$$K(\mathbf{R},\mathbf{R}')=W(\mathbf{R})D(\mathbf{R},\mathbf{R}')W^{-1}(\mathbf{R}') . \tag{4.31}$$

If we maintain for f the definition $f=\phi\psi_T$ and introduce correspondingly a new distribution $g=\phi\psi_G$, relative to the guidance wave function, one can rewrite Eq. (4.20) as

$$g(\mathbf{R})=(E+V_0)\int d\mathbf{R}'D(\mathbf{R},\mathbf{R}')g(\mathbf{R}') \tag{4.32}$$

and, of course,

$$f(\mathbf{R})=W(\mathbf{R})g(\mathbf{R}) . \tag{4.33}$$

Equation (4.32) must be iterated, starting from a suitable initial distribution. The best that one can choose is to start from the fixed-node distribution $g_{FN}=\phi_{FN}\psi_G$, obtained, for instance, from a previous calculation with guidance function ψ_G. To this fixed-node distribution corresponds an initial g,

$$g_0(\mathbf{R})=\sigma_0(\mathbf{R})|g_{FN}(\mathbf{R})|\equiv\sigma_0(\mathbf{R})|g(\mathbf{R})| \tag{4.34}$$

where

$$\sigma_0(\mathbf{R})=W(\mathbf{R})/|W(\mathbf{R})|=\mathrm{sgn}[\psi_T(\mathbf{R})] . \tag{4.35}$$

From the computational point of view, one can just begin iterating Eq. (4.32) starting from $g=|g_0|$, and assigning to each new walker a *counter* in which is stored the sign σ_0 of the initial fixed-node parent. In this manner, only positive distributions enter the random walk. The final distribution $f=\phi\psi_T$ is then easily obtained from the walker population corresponding to the final g by assigning to each walker a weight and a sign according to $W(\mathbf{R})\sigma_0$, where $\mathbf{R}$ is the position of the walker and σ_0 is the sign associated with the position of the initial fixed-node parent, at the beginning of the random walk. This immediately follows from Eqs. (4.32)–(4.34).

Once the nodal relaxation has been performed, the fermionic ground-state energy can be evaluated via the local energy estimator, introduced with Eq. (4.8), which in the present case can be written as

$$E_0=\frac{\sum_i W(\mathbf{R}_i)\sigma_0 E_L(\mathbf{R}_i)}{\sum_i W(\mathbf{R}_i)\sigma_0} . \tag{4.36}$$

We stress once again that, in applying the nodal relaxation method to practical calculation, it is essential to start from a very good guess for the fermionic ground state, in order to minimize the length of the random walk associated with the relaxation of the nodes. In fact, during the evolution of the modulus of the wave function, the fermionic signal decreases in favor of the bosonic component. This leads, for instance, to an exponential growth in the variance of the energy with respect to its average value, as can be seen from the definition of average implied by the local energy estimator of Eq. (4.36) (Kalos, 1984; Schmidt and Kalos, 1984).

Finally, we wish to comment on the choice of the guidance wave function. ψ_G should be sufficiently close to $|\psi_T|$ to ensure an efficient sampling of configuration space, ψ_T having been chosen so as to be a good approximation to the exact ground state. However, in the case in which nodal relaxation is performed, other considerations come into play. In particular, within the framework of the diffusion Monte Carlo method, it appears from Eqs. (4.4) and (4.5) that a zero of the guidance function corresponds to an infinitely repulsive force acting on the walkers. This means that the walkers are pushed away from the nodal surfaces of ψ_T and cannot cross them. In other words, the statistical system associated with the walkers is nonergodic, in that the walkers cannot redistribute themselves among the various domains determined by the nodal surfaces. On the other hand, within the Green's-function Monte Carlo procedure, the vanishing of ψ_G yields an excessive branching in the walker generation (Ceperley and Alder, 1984). In either case, a simple way to remedy this inconvenience is to take $\psi_G(\mathbf{R})=|\psi_T(\mathbf{R})|[1+s(\mathbf{R})]$, where $s(\mathbf{R})$ is a nonnegative function which is very small away from nodal surfaces and vanishes at infinity. Near a nodal surface, however, $s(\mathbf{R})$ behaves in such a way as to make $\psi_G(\mathbf{R})$ small but finite. A reasonable choice of $s(\mathbf{R})$ is obtained by compromising between reduction of branching and efficiency of the sampling (Ceperley and Alder, 1984).

D. Monte Carlo computer experiments on phase transitions in uniform interacting-electron assembly

The ground-state energy of a uniform interacting-electron assembly has been computed by Ceperley and Alder (1980) with the diffusion Monte Carlo method described in Sec. IV.A. In particular, these authors have calculated the ground-state energy for four distinct phases of this system of charged particles, at various den-

sities. They have considered (a) the unpolarized Fermi fluid, (b) the fully polarized Fermi fluid, (c) the Bose fluid, and (d) the Bose crystal on a bcc lattice. With this information, which can be regarded as the most accurate to date, they were able to predict the transitions between the various phases with reasonable accuracy.

For each phase, the calculations were performed by first generating fixed-node wave functions, or more precisely the corresponding random-walker populations, and then applying to such fixed-node distributions the nodal relaxation scheme discussed in Sec. IV.C. The trial wave functions for the Fermi phases were chosen as a product of Slater determinants, one for each spin-projection population, times a Jastrow factor ensuring the cusp condition as any two electrons approach each other. The Slater determinants were constructed from plane waves with the wave vector lying within the Fermi sphere. Of course, at given density the Fermi wave vector of the fully polarized electron fluid is $2^{1/3}$ larger than that of the unpolarized system. For the crystalline phase, the one-particle orbitals were chosen as Gaussians centered on the lattice sites with a width chosen variationally.

The analysis of the convergence of the nodal relaxation shows that in the present case the Hartree-Fock nodes, which were employed in the calculations, constitute a good approximation to the nodes of the exact wave function. In fact, it was found that the convergence of the relaxation process was relatively quick. The effect of the finite number of particles and finite time step on the results of the calculations was also systematically studied, and extrapolations to infinite number of particles and zero time step were performed. The systematic error originating from the finiteness of the *sample* was found to be one order of magnitude larger than the statistical error, in spite of the fact that the interactions between the particles and their images in the periodically extended space were taken into account with an Ewald summation procedure (see, e.g., Ceperley, 1978) to eliminate the major surface effect.

The results of Ceperley and Alder for the charged Fermi and Bose systems are fully summarized in Table I. A more direct interpretation of their findings is obtained

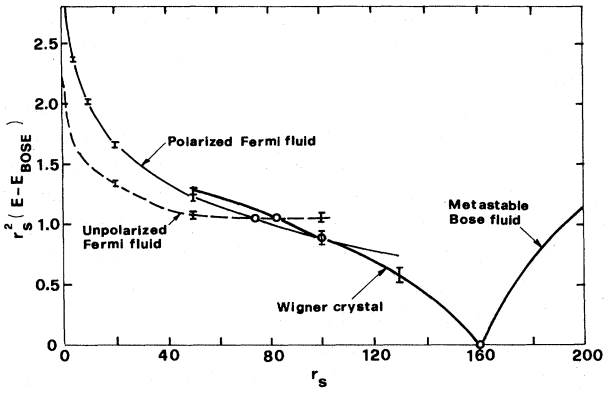

FIG. 7. Energy of the four phases studied relative to that of the lowest boson state times r_s^2 in rydbergs vs r_s in Bohr radii. Below $r_s=160$, the Bose fluid is the most stable phase; above, the Wigner crystal is most stable. The energies of the polarized and unpolarized Fermi fluid are seen to intersect at $r_s=75$. The polarized (ferromagnetic) Fermi fluid is stable between $r_s=75$ and $r_s=100$, the Fermi Wigner crystal above $r_s=100$, and the normal paramagnetic Fermi fluid below $r_s=75$. From Ceperley and Alder (1980).

from Fig. 7 where the quantity $r_s^2(E-E_{\text{Bose}})$ is plotted against r_s. Thus the energy of each phase is referred to the Bose ground state. The two curves corresponding, respectively, to the paramagnetic ground state and to the Wigner crystal intersect when $r_s\approx 80$ Bohr radii. Interest in the fully polarized or ferromagnetic state was indicated by Bloch's work within the Hartree-Fock approximation (Bloch, 1928). Bloch's theory represents the simplest example of spin-density-functional theory. Of course, it is now well known that Hartree-Fock theory predicts too readily the existence of ferromagnetism. This is because it correlates parallel-spin electrons essentially correctly through the Fermi hole, whereas antiparallel-spin electrons are uncorrelated. Thus the energy of the fully ferromagnetic state is predicted more accurately than that of the paramagnetic state. In particular, Bloch's theory leads to ferromagnetism for $r_s>6$. This is only a slightly larger r_s than for metallic cesium,

TABLE I. Ground-state energy of the charged Fermi and Bose systems. r_s is the Wigner-sphere radius in units of Bohr radii. Energies are in rydbergs, and the digits in parentheses represent the error bar in the last decimal place. The four phases are the paramagnetic or unpolarized Fermi fluid (PMF); the ferromagnetic or polarized Fermi fluid (FMF); the Bose fluid (BF); and the Bose crystal with a bcc lattice (bcc).

r_s	PMF	FMF	BF	bcc
1.0	1.174(1)	...	...	...
2.0	0.0041(4)	0.2517(6)	−0.4531(1)	...
5.0	−0.1512(1)	−0.1214(2)	−0.21663(6)	...
10.0	−0.10675(5)	−0.1013(1)	−0.12150(3)	...
20.0	−0.06329(3)	−0.06251(3)	−0.06666(2)	...
50.0	−0.02884(1)	−0.02878(2)	−0.02927(1)	−0.02876(1)
100.0	−0.015321(5)	−0.015340(5)	−0.015427(4)	−0.015339(3)
130.0	...	...	−0.012072(4)	−0.0123037(2)
200.0	...	...	−0.008007(3)	−0.008035(1)

the lowest electron-density metal. There is no sign of a tendency to ferromagnetism in the physical properties of this metal.

In fact, as a comparison of the curves from computer experiments displayed in Fig. 7 shows, the ferromagnetic state does not become stable with respect to the paramagnetic state until $r_s > 70$, indicating the vital importance of electron correlation in discussing this magnetic transition. This ferromagnetic state intersects the Wigner crystal at $r_s \approx 100$. Around such values of r_s the Bose and Fermi crystals differ in energy by an amount which is less than 1.0×10^{-6} rydbergs.

While Ceperley and Alder point out that their computer studies need refinement, there can be little doubt that the Wigner crystal becomes stable in the range $70 < r_s < 100$, and this, of course, is very valuable information. We notice that one area of obvious importance, if the Wigner electron crystal is to be unambiguously identified in three dimensions, is the question of the temperature at which melting of the electron crystal will occur.

E. Calculation of correlation energy for small molecules

Configuration-interaction calculations have been able, in the past, to account typically for about 80% of the correlation energy of molecules such as water (see, for example, Meyer, 1971 and Rosenberg and Shavitt, 1975). However, interesting chemistry occurs on an energy scale of only a fraction of the correlation energy. For example, the O-H bond strength in water is about 50% of the correlation energy. Thus the correlation energy computed using large CI wave functions differs from the exact (nonrelativistic, Born-Oppenheimer) energy by an amount of this same order of magnitude. Improving the CI results can be difficult, since convergence to the exact result is slow and can be nonuniform. Nevertheless, present-day state-of-the-art CI calculations yield whenever possible very accurate energy estimates (Mårtensson-Pendrill *et al.*, 1991) and to date still provide the yardstick against which all other calculations are measured. The numerical effort involved in CI calculations for a system of N electrons increases with a power of N which is between 4 and 5.

The quantum Monte Carlo method, at least in principle, appears to be free of the limitations inherent to an expansion procedure. In practice, in the absence of a stable algorithm to implement nodal relaxation, optimizing the nodes of the trial wave function becomes a crucial issue. Moreover, treating molecules with large nuclear charges Z by QMC may require very large computational times, even larger than in CI. In fact, though Reynolds *et al.* (1982) optimistically estimated that the computational effort needed in QMC would increase only as the third power of the number of electrons, subsequent and more careful estimates yield, for an atom with nuclear charge Z, a computational effort that increases either as $Z^{5.5}$ (Ceperley, 1986) or as $Z^{6.5}$ (Hammond *et al.*, 1987).

The quantum Monte Carlo method was developed and used primarily in the fields of nuclear and condensed-matter theory (cf. Sec. IV.D on jellium). However, subsequent chemical calculations have been performed (Anderson, 1975, 1976, 1980; Mentch and Anderson, 1981; Moskowitz and Kalos, 1981; Alder *et al.*, 1982; Moskowitz *et al.*, 1982a, 1982b; Ceperley and Alder, 1984; Moskowitz and Schmidt, 1986). In the following we shall briefly review some of these calculations. In particular, we shall illustrate the quality of calculations performed (a) with diffusion Monte Carlo, (b) with the Green's-function Monte Carlo, (c) within the fixed-node approximation, and (d) with allowance for nodal relaxation. We shall also comment again on limitations and possible developments of QMC.

The DMC method has been applied by Reynolds *et al.* (1982) to the calculation of the ground-state energy of some small molecules, H_2, LiH, Li_2, H_2O, within the fixed-node approximation. Trial wave functions of different sophistication were considered by these authors so as to show the importance of ψ_T on the efficiency of the sampling. All their importance functions were in the form of a product: a Slater determinant for each of the two groups of electrons with given spin projection times a correlation factor of Jastrow type. Of course, the Slater determinants were taken in such a way as to ensure the symmetry associated with the particular choice of the total spin projection, whereas the Jastrow factor was such as to reproduce the correct cusp behavior of the wave function as the electrons approach each other. They have considered three kinds of trial wave functions corresponding to Slater determinants constructed, respectively, from (a) a minimal basis set of Slater-type atomic orbitals, (b) a somewhat enhanced basis set and/or an optimized version of (a) and (c) localized Gaussian orbitals. In case (c) the Jastrow factor contained additional terms to reproduce also the cusp behavior associated with the electron-nuclear Coulomb attraction: this should have the effect of making the local energy associated with ψ_T even smoother.

In Table II, the fixed-node (FN) quantum Monte Carlo ground-state energy for some molecules is reported for the three choices of ψ_T listed above. Reported also for comparison are the energies obtained with the Hartree-Fock (HF) approximation, the best CI calculations, and the *exact* clamped nuclei or Born-Oppenheimer approximation, in the usual nonrelativistic framework afforded by the many-electron Schrödinger equation. All the energies are in hartrees. It is clear that, with the exception of the water molecule, in all cases the fixed-node energy accounts for most of the correlation energy. There are improvements in going from simpler to more sophisticated wave functions, so that with the best trial wave function (III) the fixed-node energy accounts for 95% or more of the correlation energy. It should be noted that in the case of the hydrogen molecule the ground-state wave function has no nodes. Therefore differences between fixed-node and exact energies of H_2, which are beyond

TABLE II. Total ground-state energy (in hartrees) of some small molecules (from Reynolds *et al.*, 1982). The figure in parentheses is the statistical error. The various symbols are explained in the text.

	H_2	LiH	Li_2	H_2O
HF	−1.1336	−7.987	−14.872	−76.0675
FN-I	−1.1745(8)	−8.047(5)	−14.985(5)	−76.23(2)
FN-III		−8.059(4)	−14.991(7)	−76.377(7)
FN-III	−1.174(1)	−8.067(2)	−14.990(2)	
Best CI	−1.1737	−8.0647	−14.903	−76.3683
Exact	−1.17447	−8.0699	−14.9967	−76.4376

the statistical error, give a measure of the numerical error associated with the use of a finite time step in the diffusion Monte Carlo calculations. In the case of the water molecule, it seems that none of the trial functions that were used is of especially good quality. In fact, in such a case only about 80% of the correlation energy is accounted for by the fixed-node calculations.

Reynolds *et al.* (1982) have also performed fixed-node calculations for the ground-state energy of the lithium diatomic molecule at various internuclear distances around the equilibrium one. The results of such calculations, based on a ψ_T of type II, are reported in Table III, together with the Hartree-Fock and the exact energy. It is found that 90% or more of the correlation energy is obtained also in this case.

As noted by Reynolds *et al.* (1982), the Born-Oppenheimer approximation, adopted throughout their work, can also be relaxed. This is achieved by allowing the nuclei, as well as the electrons, to diffuse. The diffusion constant for each nucleus is then $\hbar/2M$, where M denotes the nuclear mass. Thus the nuclei diffuse considerably more slowly than the electrons, and this makes the calculation longer.

Thus it is found that by using relatively simple trial functions ψ_T and making only a modest computational effort, one can obtain with the fixed-node QMC at least as much, and often more, of the correlation energy than proves possible by CI calculations to date, for simple molecules.

Fixed-node calculations for small molecules using the domain Green's-function (DGF) method have been performed by Moskowitz and Schmidt (1986). As these authors stress, the use of the DGF method is free of the systematic error introduced in the DMC by the finite time step. Here we shall just briefly comment on their results.

TABLE III. Ground-state energies (in hartrees) at selected nuclear separations for Li_2. The symbols are as in Table I. Typical statistical uncertainty on the fixed-node results is 0.005 hartrees.

r (bohr)	HF	FN-II	Exact
3	−14.786	−14.905	−14.915
4	−14.853	−14.968	−14.983
5.05 (equil.)	−14.872	−14.991	−14.997
6	−14.869	−14.985	−14.992
7	−14.859	−14.976	−14.982

Among the systems that they consider are the LiH molecule, the Be atom, and the BeH_2 molecule. With their calculations they are able to reproduce ground-state correlation energies within chemical accuracy, i.e., a few percent, when using the best trial functions. The same degree of accuracy is also found in the prediction of excitation energies for the Be atom and the energy barrier for insertion of Be in H_2.

It should be stressed once again that the quality of fixed-node energies depends on the capability of the chosen trial wave function to reproduce the nodal surfaces of the exact ground state. Thus, while the fixed-node approximation yields upper bounds to the exact energy, the systematic optimization of such results does not appear to be easy. In this respect the nodal relaxation technique, which was developed by Ceperley and Alder (1980) for the electron gas in the first instance, may prove valuable. One has to keep clearly in mind, though, that such a technique only gives transient estimates for the energy. In other words, if the relaxation is performed for times too long, it becomes intrinsically unstable, with the interesting signal that decreases exponentially whereas the noise remains constant. Thus the nodal relaxation technique crucially depends on the availability of a good starting guess for the ground-state wave function, and this may be provided by a preliminary (or, in actual practice, contemporary) fixed-node calculation.

Ceperley and Alder (1984) have performed further calculations on some of the small molecules previously considered with the DMC method, improving on them in two ways. They have changed to Green's-function Monte Carlo, utilizing a technique introduced by Ceperley (1983), to sample the exact Green's function, thus eliminating any error associated with the use of a finite time step. Further, they have implemented the nodal relaxation. In these new calculations they have also considered the H_3 molecule. Below, we shall briefly review their study as an example of how nodal relaxation can work. Since we have already described in some detail the main points of the nodal relaxation method, we shall merely present their results for the ground-state energy of the molecules considered. We shall also try to exemplify a bit the problem of the *convergence* of the nodal relaxation. For these calculations, with the exception of the H_2O molecule, trial functions of type III as used in the work of Reynolds *et al.* (1982) were employed. For H_2O a more sophisticated ψ_T was used. We refer the in-

terested reader to the original paper by Ceperley and Alder (1984) for the details of their trial functions.

In Table IV we report the ground-state energy for LiH, Li_2, H_2O, and for three different configurations of H_3 denoted by H_3(I), H_3(II), and H_3(III). At first glance, the nodal relaxation appears to be able in all cases to bring down the fixed-node energy so as to agree with the exact energy. However, a few comments are necessary. It is true that the relaxed-node energies coincide with the exact ones within the statistical error. Nevertheless, the statistical error increases with increasing total energy. In addition, as has already been mentioned, the nodal relaxation can only provide transient estimates of the fermionic ground-state energy. Therefore it appears necessary to examine the convergence of the nodal relaxation in detail. To this end one can consider the total energy as a function of the generation number, starting from the first generation after the beginning of nodal release. Such curves for two typical cases are shown in Figs. 8–10. In Fig. 8 the relaxing of the total energy for LiH is shown. It is clear that in this case one can confidently speak of convergence. We stress that in the figure are also reported the results of runs in which the trial wave function was deoptimized to show how this destroys the convergence. The case of H_2O is illustrated in Fig. 9. Although the relaxed energy at the end of the run is in agreement with the exact energy, within the statistical uncertainty, there is no indication that convergence was reached, in that the slope of the energy curve does not seem to diminish.

A better way of studying the convergence of the nodal relaxation is to look at the energy difference between successive generations. Of course, a sign of convergence should be the vanishing of such a quantity after a sufficient number of generations. This quantity can also be evaluated more accurately than the total energy itself, as discussed by Ceperley and Alder (1984). In Fig. 10 the difference in release-node energy is shown for LiH. It is clear that with a good trial wave function the node relaxation can be considered to be converged. However, in the case of H_2O, reported in Fig. 11, it is not possible to say much, since the error bars increase too fast with the generation number even in the difference calculation.

The conclusion that can be drawn from the above discussion is that whereas the nodal relaxation appears to work well with light molecules, there are still problems

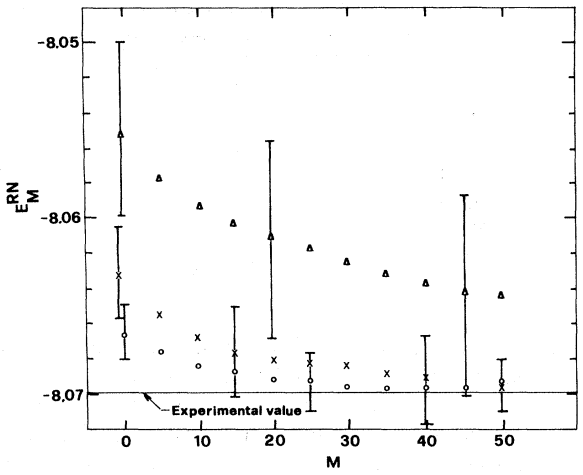

FIG. 8. Energy (in hartrees) vs the number of generations since node release for the molecule LiH. The results for three different trial functions are shown. (○) indicates the results obtained with the best trial function. The parameters in the other two trial functions were deliberately deoptimized to raise the fixed-node energy. From Ceperley and Alder (1984).

with the heavier ones. This is related to the fact that in the heavier molecules, because of the larger nuclear charges Z, the total energies are also larger and hence so are the error bars. Moreover, with increasing Z, the difference between the Bose and Fermi ground-state energy increases and, correspondingly, the rate (exponential) at which the Bose component obscures the fermionic one.

A number of ways to partially improve the QMC computations for heavier molecules are listed by Ceperley and Alder (1984). One way is based on a different treatment of inner electrons, possibly by means of pseudopotentials, so as to deal, in practice, with an equivalent problem with lower Z. Another way considers the possibility of deleting all the random walks that frequently cross the nodes. They also cite the possibility of directly calculating energy differences by means of correlated random walks. To date, practical calculations of heavier atoms and molecules, within the fixed-node approximation, have mainly exploited the separation of electrons in core and valence, followed by a different treatment of the two kinds of electrons (Hammond *et al.*, 1987; Hurley and Christiansen, 1987; Hammond *et al.*, 1988; Yoshida and Iguchi, 1988; Bachelet *et al.*, 1989). The use of pseu-

TABLE IV. Comparison of fixed-node and relaxed-node ground-state energies (in hartrees) with CI and exact results. RN indicates the relaxed-node energy, and the other symbols are as in Tables I and II. Δ is the difference $E_{FN}-E_{RN}$.

Molecule	FN	RN	Δ	Exact	CI
H_3(I)	−1.6581(3)	−1.6591(1)	0.0009(2)	−1.65919	−1.65876
H_3(II)	−1.6239(3)	−1.6244(3)	0.0005(2)	−1.62451	−1.62337
H_3(III)	−1.6606(2)	−1.6617(2)	0.0011(2)	−1.66194	−1.66027
LiH	−8.067(1)	−8.071(1)	0.004(1)	−8.0705	−8.0690
Li_2	−14.990(2)	−14.994(2)	0.004(1)	−14.9967	−14.903
H_2O	−76.39(1)	−76.43(2)	0.04(1)	−76.437	−76.368

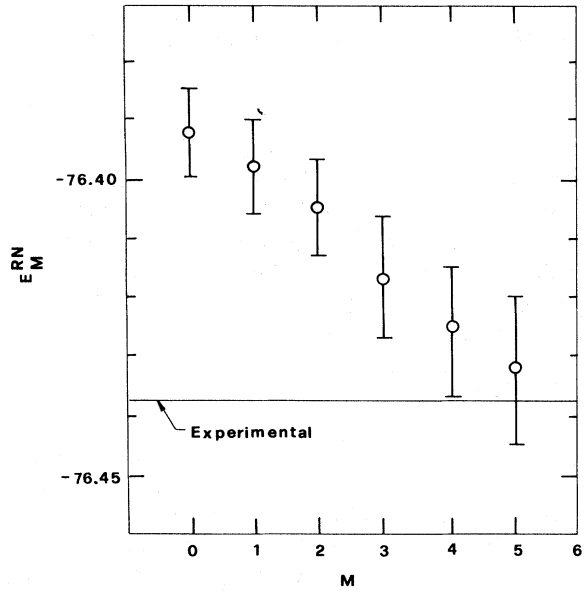

FIG. 9. Energy (in hartrees) vs the number of generations since node release for the molecule H_2O. From Ceperley and Alder (1984).

dopotentials to achieve the core-valence separation introduces, however, a new complication: good pseudopotentials are nonlocal, and this is in conflict with key aspects of QMC. To overcome this complication, workers have resorted to two tricks: either the nonlocal potentials are *made local* by suitable approximations (Hammond *et al.*, 1987; Hurley and Christiansen, 1987; Yoshida and Iguchi, 1988), or they are transformed into local ones by introducing appropriate pseudo-Hamiltonians (Bachelet *et al.*, 1989). A different approach has also been proposed and tested, in which core and valence electrons are both described in terms of wave functions, with the core, however, being treated variationally while the important valence electrons are treated by QMC (Hammond *et al.*, 1988).

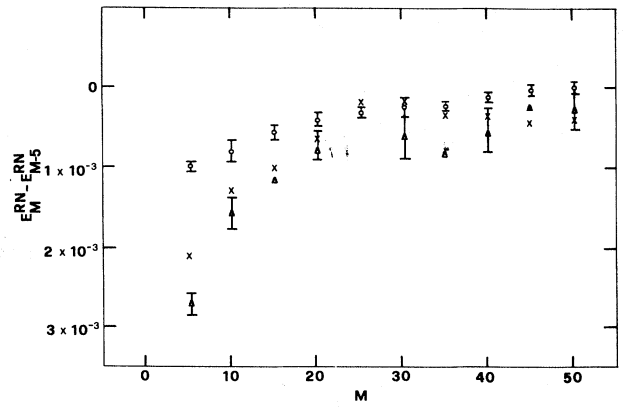

FIG. 10. Change in release-node energy (in hartrees) every five generations since node release for the molecule LiH. From Ceperley and Alder (1984).

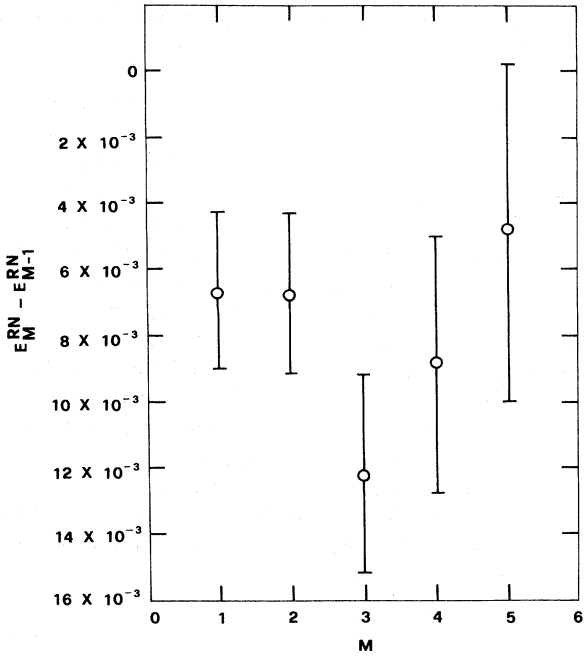

FIG. 11. Change in release-node energy (in hartrees) every five generations since node release for the molecule H_2O. From Ceperley and Alder (1984).

The severe limitation imposed on QMC calculations by the big increase with Z of the computation time remains an open problem, even though improved diffusion Monte Carlo algorithms (Umrigar *et al.*, 1991) may allow time steps considerably larger than in the past, thus partially alleviating the slowing down of calculations. In fact, the attempts mentioned above to overcome such a slowing down with a core-valence separation still appear far from developing into standard, transferable algorithms. On the other hand, even though the use of sophisticated, specifically tailored wave functions may allow very accurate predictions of the correlation energy in fixed-node calculations (Umrigar *et al.*, 1991), nodal relaxation remains very difficult to implement, because of the lack of a stable algorithm. Thus the fermion sign problem and the computational slowing down for species with large Z remain open challenges for the quantum Monte Carlo treatment of many-electron systems.

F. Auxiliary-field quantum Monte Carlo method and Hubbard model

The central idea of the auxiliary-field quantum Monte Carlo (AFQMC) method, as we have already anticipated, is to exactly rewrite the propagator of a many-particle system—with two-body interactions—in terms of a propagator for independent particles interacting with auxiliary external fields. While this procedure introduces the need for averaging over the values taken by such ex-

tra fields, it permits the use of well-established techniques to treat the propagator for independent particles. The strategy is relatively simple and contains three main steps: (a) find the appropriate transformation that replaces the coupling between the particles with a coupling to suitably chosen classical fields; (b) solve the new independent particle problem; i.e., calculate the trace (partition function) or a suitable matrix element of the propagator; (c) perform the average over the auxiliary fields, usually with techniques borrowed from classical statistical mechanics. For the sake of simplicity, rather than considering the general case of an arbitrary Hamiltonian with quadratic interactions (see, e.g., Sugiyama and Koonin, 1986; Negele and Orland, 1988), here we shall concentrate on the specific case of the Hubbard model, for which we shall then discuss some applications.

The basic relation that allows for the introduction of the auxiliary fields is the Hubbard-Stratonovich (HS) identity (Stratonovich, 1957; Hubbard, 1959) valid for any Hermitian operator $\hat{O}$,

$$e^{(1/2)\alpha^2\hat{O}^2}=\frac{1}{\sqrt{2\pi}}\int_{-\infty}^{\infty}dx\, e^{-(1/2)x^2}e^{-\alpha x\hat{O}}\ , \tag{4.37}$$

or appropriate extension of it (see below). The Hubbard Hamiltonian of Eq. (4.10) contains a one-body term, $K=\sum_{ij\sigma}t_{ij}a_{i\sigma}^{+}a_{j\sigma}$, and a two-body interaction $V=U\sum_i n_{i\uparrow}n_{i\downarrow}$. Therefore it appears to be a good candidate for the HS transformation. However, the propagator $e^{-\beta H}$ contains the sum H_0+V, rather than merely V. Here $H_0=K-\mu\sum_{i\sigma}a_{i\sigma}^{+}a_{i\sigma}$. The trick for circumventing this difficulty is to resort to the Trotter formula,

$$\begin{aligned}e^{-\beta(H_0+V)}&=\prod_{r=1}^{L}e^{-\varepsilon(H_0+V)}\\&=\prod_{r=1}^{L}e^{-\varepsilon H_0}e^{-\varepsilon V}+O(\varepsilon)\ ,\end{aligned} \tag{4.38}$$

with $\varepsilon=\beta/L$, so that the exponential of V appears explicitly. In fact, V still needs some rearranging. One possibility is to rewrite $e^{-\varepsilon V}$—in each of the time slices generated by the Trotter formula—using the relation (Hirsch, 1983)

$$n_{i\uparrow}n_{i\downarrow}=-\tfrac{1}{2}(n_{i\uparrow}-n_{i\downarrow})^2+\tfrac{1}{2}(n_{i\uparrow}+n_{i\downarrow})\ , \tag{4.39}$$

which is valid for fermions ($n_{i\sigma}^2=n_{i\sigma}$). Then, use of the HS transformation in Eq. (4.38) and elementary manipulations yield the propagator in a new form,

$$\begin{aligned}U(\beta)&=e^{-\beta H}\\&=\left[\frac{\varepsilon}{2\pi}\right]^{NL/2}\\&\quad\times\int\prod_{r=1}^{L}\prod_{i=1}^{N}dx_{ri}e^{-(\varepsilon/2)x_{ri}^2}\prod_{r'=1}^{L}e^{-\varepsilon h_{r'}(x)}\ ,\end{aligned} \tag{4.40}$$

valid to order ε, with

$$h_r(x)=H_{0r}+\sum_i\left[\sqrt{U}x_{ri}(n_{ri\uparrow}-n_{ri\downarrow})+\frac{U}{2}(n_{ri\uparrow}+n_{ri\downarrow})\right] \tag{4.41}$$

and N the number of sites of the finite lattice on which the Hubbard model is considered. It is evident that the Hamiltonian $h_r(x)$ contains only one-body operators: in particular, it describes independent particles moving in an external field $\sqrt{U}x_{ri}$. Thus, through a Gaussian averaging, the imaginary-time propagator $U(\beta)$ is related to a new propagator for independent particles,

$$U_\varepsilon(\beta,x)=\prod_{r=1}^{L=\beta/\varepsilon}e^{-\varepsilon h_r(x)}\ . \tag{4.42}$$

A number of comments are in order. The accuracy of Eq. (4.40) increases with increasing $L=\beta/\varepsilon$, and this alternative representation of the propagator only becomes exact in the limit $\varepsilon\to 0$ ($L\to\infty$). However, one can study systematically such a convergence and accordingly estimate the systematic error introduced by a finite Trotter time ε. The reader will have noted the presence in Eqs. (4.40) of a time index denoted by r. This new labeling simply keeps track of the Trotter time slice.

As we have anticipated, quantities that one typically wants to calculate are the partition function $Z=\mathrm{Tr}U(\beta)$ or a *projected* partition function $Z_T=\langle\Phi_T|U(\beta)|\Phi_T\rangle$, where Φ_T is a trial wave function nonorthogonal to the ground state. In either case, for $\beta\to\infty$ one obtains a limiting behavior $Z(Z_T)\propto e^{-\beta E_0}$. Thus one can obtain E_0 as

$$E_0=-\lim_{\beta\to\infty}\frac{1}{\beta}Z(\beta)=-\lim_{\beta\to\infty}\frac{1}{\beta}Z_T(\beta)\ . \tag{4.43}$$

From Eqs. (4.40) and (4.41) it is clear that the evaluation of Z requires that of

$$\tilde{Z}(x)=\mathrm{Tr}U_\varepsilon(\beta,x)\ . \tag{4.44}$$

This can be evaluated (Blankenbecler *et al.*, 1981) in terms of a determinant involving the matrices associated with the Hamiltonians $h_r(x)$ of Eq. (4.41). Once $\tilde{Z}(x)$ is known, the problem of calculating Z is reduced to that of evaluating a multidimensional integral over the variables $\{x_{ri}\}$. In fact, one readily obtains

$$Z=\int dx\, e^{-\beta\tilde{U}(x)}\mathrm{sgn}(\tilde{Z}(x))\ , \tag{4.45}$$

where

$$\int dx\equiv\left[\frac{\varepsilon}{2\pi}\right]^{NL/2}\int\prod_{r=1}^{L}\prod_{i=1}^{N}dx_{ri} \tag{4.46}$$

and

$$\tilde{U}(x)\equiv\frac{1}{2L}\sum_{r=1}^{L}x_{ri}^2-\frac{1}{\beta}\ln|\tilde{Z}(x)|\ . \tag{4.47}$$

Thus the problem of calculating the partition function for a quantum system is reduced to the classical problem

of calculating a configurational integral. We shall merely note that numerical problems may, however, arise from the possible presence of nodal surfaces in the function $\tilde{Z}(x)$. These can give (a) problems of ergodicity in sampling the integral of Eq. (4.44) as well as (b) problems of signal-to-noise ratio if Z results from the cancellation of large contributions of opposite sign. This is a manifestation of the so-called fermion sign problem.

The considerations above, and, in particular, Eqs. (4.44)–(4.46), remain valid if one calculates a projected partition function—the only difference being that Z and $\tilde{Z}(x)$ are replaced by Z_T and $\tilde{Z}_T(x) = \langle \Phi_T | U_\varepsilon(\beta,x) | \Phi_T \rangle$, respectively. Appropriate techniques are available (Sugiyama and Koonin, 1986; see also Sorella, 1989) to evaluate $Z_T(x)$. With manipulations similar to those reviewed above, it is also possible to reduce the calculation of relevant correlation functions to that of pseudoclassical averages. It seems proper at this point to add that, particularly for the Hubbard Hamiltonian, it has proved possible (Hirsch, 1983) to write a discrete transformation of the HS type, i.e.,

$$e^{-\varepsilon U n_{i\uparrow} n_{i\uparrow}} = \frac{1}{2} \sum_{\sigma=\pm 1} e^{-\varepsilon[J\sigma(n_{i\uparrow}-n_{i\downarrow})+U(n_{i\uparrow}+n_{i\downarrow})/2]} , \qquad (4.48)$$

with $\cosh(\varepsilon J) = e^{\varepsilon U/2}$. This transformation maps the quantum Hubbard problem onto an equivalent classical problem where one has to sample over Ising variables, rather than continuous ones. According to Hirsch (1986), in calculations using the transformation of Eq. (4.47), the sign problem is not severe.

To give a practical illustration of the AFQMC, we shall discuss recent work on the 2D Hubbard model, stimulated by its possible relevance to the high-T_c superconductors. We shall not attempt here to give an exhaustive review, and therefore the interested reader is urged to consult the original papers mentioned below for a detailed discussion and further references.

Hirsch and Tang (1989) have studied the 2D Hubbard model with nearest-neighbor hopping for lattices as big as 8×8 and for imaginary times up to $\beta = 20$, in units in which the hopping energy $-t = -1$. They have performed AFQMC simulations based on the sampling of the partition function Z for different values of the coupling U and of the filling ρ—defined as the ratio between the number of electrons N_e and the number of sites in the lattice N, $\rho = N_e/N$. Because of electron-hole symmetry, one can take $\rho \leq 1$. The doping can be suitably defined as $\delta = 1-\rho$. Since the lattice can accommodate $2N$ electrons, $\rho = 1$ corresponds to half filling and, similarly, $\rho = 0.5$ to a quarter filling. Hirsch and Tang have looked especially into the magnetic properties of the system, which can be characterized by the magnetic structure factor

$$S(\mathbf{q}) = \frac{1}{N} \sum_{ij} e^{i\mathbf{q}\cdot(\mathbf{l}_i - \mathbf{l}_j)} \langle (n_{i\uparrow} - n_{i\downarrow})(n_{j\uparrow} - n_{j\downarrow}) \rangle \qquad (4.49)$$

and, in particular, by its value at the wave vector $\mathbf{q}_m = (\pi,\pi) \equiv \pi$. They find that at half filling the magnetic structure factor exhibits a sharp peak at $\mathbf{q}_m$. Such a peak, which is shown in Fig. 12, tends to become more and more pronounced with increasing lattice size or coupling U. Also apparent—from the same figure—is the saturation of $S(\pi)$ with increasing simulation time β. In fact, as the time becomes shorter, the drop in $S(\pi)$ becomes more and more pronounced for larger lattices and couplings. The presence of such a peak in $S(\mathbf{q})$ is interpreted as a sign of antiferromagnetic long-range order. As they move from $\rho = 1$, they find a rapid suppression of such an ordering, as can be seen from Fig. 13, and they conjecture that the antiferromagnetic order disappears immediately away from half filling. Hirsch and Tang also find that at low temperatures (long imaginary times) the properties of the 2D Hubbard model at half filling are well described by a spin-wave theory with renormalized local moment and spin-wave velocity.

The results of Hirsch and Tang are consistent with those of recent MC simulations (Reger and Young, 1988) of the two-dimensional antiferromagnetic Heisenberg model with which the two-dimensional Hubbard model at half filling is equivalent for large U. Moreover, they are fully confirmed by independent investigations on the Hubbard model. In Fig. 14 we show the results of White *et al.* (1989) for the spin-spin correlation function

$$c(l_x,l_y) = \frac{1}{N} \sum_i \langle m(\mathbf{l}_i + \mathbf{l}) m(\mathbf{l}_i) \rangle , \qquad (4.50)$$

where $m(\mathbf{l}_i)$ is the local magnetic operator along the z axis. Clearly, while staggered spin correlations are clearly visible for half filling, these are nearly absent for the quarter-filled case. In fact, results of Sorella (1989), obtained using the projected partition function technique and Langevin dynamics to sample the pseudoclassical partition function, show that, even with a doping δ of only 12%, such correlations are practically absent. Thus

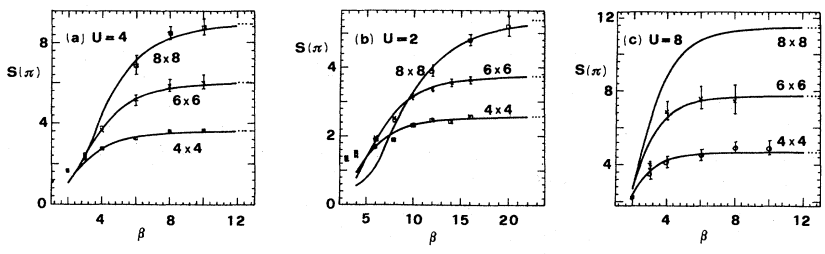

FIG. 12. Magnetic structure factor for $S(\pi) \equiv S[\mathbf{q}=(\pi,\pi)]$ vs imaginary time β for lattices of size 4×4, 6×6, and 8×8, at half filling. The solid lines are results of spin-wave theory (Hirsch and Tang, 1989). The dashed lines at the right side indicate the $T=0$ limits of the spin-wave results. From Hirsch and Tang (1989).

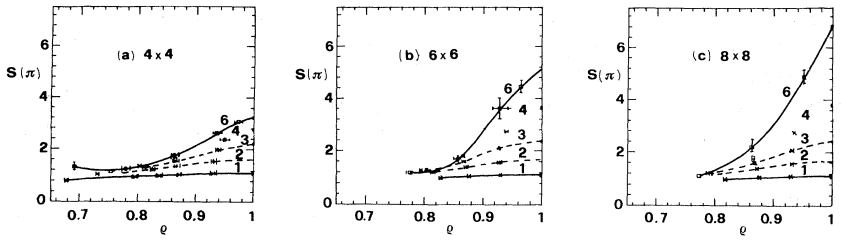

FIG. 13. Magnetic structure factor for $S(\pi)\equiv S[\mathbf{q}=(\pi,\pi)]$ vs band filling for $U=4$, with 4×4, 6×6, and 8×8 lattices at various imaginary times. The numbers next to the curves indicate β; the curves are drawn through the points to guide the eye. From Hirsch and Tang (1989).

the conjecture of Hirsch and Tang on the suppression of antiferromagnetic order away from half filling seems fully confirmed.

White *et al.* have also presented results for the single-particle momentum occupation $n(\mathbf{k})\equiv\langle n_{\mathbf{k}\sigma}\rangle = \langle a^{\dagger}_{\mathbf{k}\sigma}a_{\mathbf{k}\sigma}\rangle$. As can be seen from Fig. 15, the one-electron momentum distribution for the interacting electrons at half filling is broadened more than at a quarter filling, with respect to the noninteracting-electron case. This is also confirmed by a subsequent study by Moreo *et al.* (1990), which in addition, from an investigation of the compressibility and of the electron self-energy, provides evidence for a one-electron gap at half filling. Of course, this is consistent with the presence of antiferromagnetic long-range order. On the contrary, there is no evidence of a gap at a quarter filling where the system appears to be in a Fermi-liquid state—as is also suggested by the sharpness of the one-electron momentum distribution which more closely resembles that for noninteracting electrons. Thus one can conclude that in two dimensions the Hubbard model predicts antiferromagnetic long-range order for any finite U at half filling behaving like an insulator, whereas such order disappears on moving away from $\rho=1$ and the system behaves rather like a paramagnetic Fermi liquid.

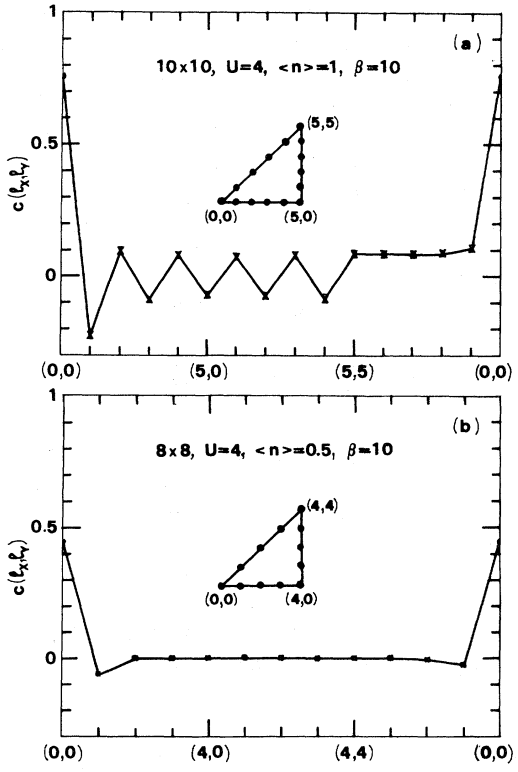

FIG. 14. Spin-spin correlation function $c(l_x,l_y)$. The horizontal axis traces out the triangular path seen in the center of the figure. Strong antiferromagnetic correlations are visible in (a), which is for a half-filled band ($\langle n\rangle\equiv\rho=1.0$), but are nearly absent in (b), which is at quarter filling ($\langle n\rangle\equiv\rho=0.5$). From White *et al.* (1989).

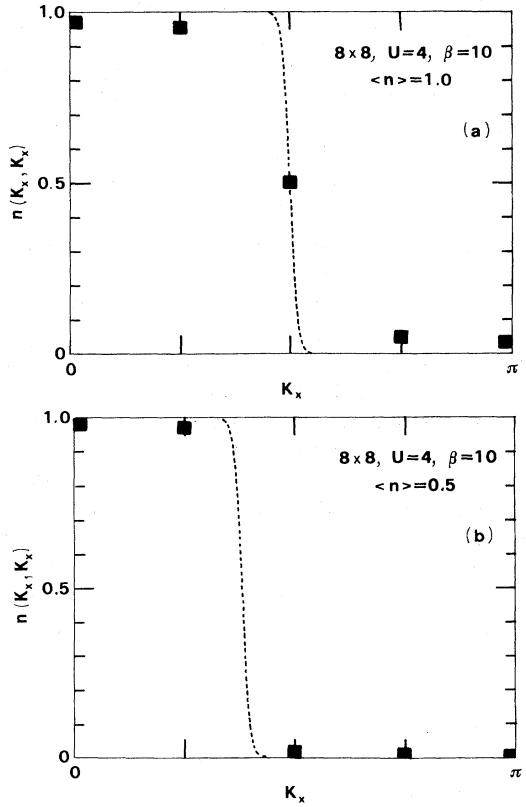

FIG. 15. Momentum distribution $n(\mathbf{k})$ for an 8×8 lattice with $U=4$ and $\beta=10$ at (a) half filling ($\langle n\rangle\equiv\rho=1.0$) and at (b) quarter filling ($\langle n\rangle\equiv\rho=0.5$). The dashed curves are the $U=0$ results. From White *et al.* (1989).

V. SUMMARY AND FUTURE DIRECTIONS

The major topics discussed in this article fall into two categories: (a) full many-body treatments of molecules and solids, and (b) simplified models, in which, however, strong correlations can be accommodated, at least in principle.

These two categories overlap in important areas. Thus (a) includes the jellium model of a metal which, in spite of its simplicity, has provided the basis for the development of the original Thomas-Fermi-Dirac method (see Gombás, 1949; March, 1957) into the theory of the inhomogeneous electron gas or, more formally, density-functional theory (Hohenberg and Kohn, 1964). Within this framework, fairly realistic calculations can now be performed on properties determined by the ground-state charge density alone for metallic, semiconducting, and insulating crystals. These calculations build the jellium results into the exchange and correlation contribution to the one-body crystal potential. While this treatment, which follows closely the pioneering work of Slater (1951) and was formalized into the current approach by Kohn and Sham (1965), is by now widely used in extensive systems, it has obvious limitations due to the forcing of the many-electron problem into a one-electron mold. One of these, the gap problem in insulators and semiconductors, is so severe that the correction to the one-body potential band gap is the order of the band gap itself (see, for example, Sham and Schlüter, 1983). To correct this, one must go back to a fully many-electron approach involving the nonlocal mass operator (Pickett, 1986; Godby *et al.*, 1988; Fiorentini and Baldereschi, 1992).

Having dealt with the way the results of the jellium model can be built into realistic calculations on molecules and solids, we turn to the second class, under (b), which is provided by Hubbard- and related Heisenberg-model Hamiltonians. These are designed to treat situations in which very strong electron-electron correlations tend to bring about site localization of electrons. Here the basic idea, at the simplest level, is to keep antiparallel electrons apart by imposing an energy penalty, U, for allowing two electrons with antiparallel spins simultaneously on a given atomic site. It is interesting that the variational wave-function approaches of Coulson and Fischer for H_2 from the quantum-chemical angle, and subsequently Gutzwiller from the standpoint of low-order density-matrix theory, address what amounts to essentially the same basic point: how to reduce the weight of ionic configurations in a molecular-orbital or band-theory approach. The strong interplay between chemical and physical points of view should be clear from the account of Sec. III, where a local approach to correlation in molecules is also given some prominence. We shall return to this interplay below.

But before doing so, we must stress here, following Sec. IV, that the very accurate correlation energy calculations have come from quantum Monte Carlo computer techniques. However, crucial input into such calculations is a trial wave function. For the jellium model, which was simulated by the above technique by Ceperley and Alder (1980), the trial function was a Slater determinant of plane waves, multiplied by a product of pairs (Bijl-Jastrow) wave function. The analytical efforts expended earlier on such wave functions, which unfortunately almost always had to invoke relatively uncontrolled approximations to allow the calculation of the appropriate low-order density matrices determining the energy, have been brought to fruition through the addition of the quantum Monte Carlo technique. But as well as the jellium results, correlation energies of small molecules are also reported in Sec. IV, together with some numerical solutions of the two-dimensional Hubbard model.

This prompts us to return to the theme raised above as to the fruitful interplay between physical and chemical ideas in treating realistic many-electron systems. This was already apparent in the early and originally largely parallel developments in the quantum chemistry of the polyenes, which anticipated, through the recognition of alternating single and double bonds (see, for example, the survey for Murrell, 1971), what solid-state physicists today call "Peierls's theorem," namely, that one-dimensional metals cannot exist. Later the exact solution of the one-dimensional Hubbard Hamiltonian by Lieb and Wu (1968; see also Kotrla, 1990) was a significant step in the study of strong correlations, though it did not allow for bond alternation. However, this has now been done in the quantitative, though admittedly approximate, work of Kajzar and Friedel (1987). In this same context, the high-T_c superconductors (see, for example, Micnas *et al.*, 1990) have had, as one by-product, to bring Pauling's theory of resonating valence bonds (RVB) back into fashion, as briefly summarized in Sec. III.E.

But, in more general terms, one question that surely remains at the heart of the theory of the high-T_c ceramic oxide superconductors is whether the chemistry of these very specific systems can in fact be subsumed within the parameter space of the currently popular two-dimensional Hubbard model. If this proved to be the case, then the system specificity already referred to must mean that high-T_c superconductivity can only be obtained in a very tiny portion of this parameter space. Certainly, the recent discussion of Anderson (1990) suggests that, already, considerable new insight is coming from low-dimensional Hubbard models, when solved in a highly accurate manner via Tomonaga-Luttinger-liquids theory. This approach, going back to Luther (1979) and taken forward in a major way by Haldane (1981), promises to have a lot to say that will be, at least, highly relevant to the normal state of high-T_c superconductors. The main point to stress here is that careful many-body analysis of interacting fermion systems reveals the possibility of two fixed points. One is the well-established Landau-Fermi-liquid theory. In this theory the interaction parameters are marginal operators around a single fixed point: essentially the free Fermi liquid [Anderson (1990), who refers to the work of Benfatto and Gallavotti

(1990)]. The Luttinger liquid was defined by Haldane (1981), who showed that a large variety of one-dimensional quantum fluids could all be solved by common techniques based on transforming to phase and phase-shift variables for the Fermi-surface excitations. As Anderson (1990) emphasizes, these systems are characterized by fractionation of quantum numbers and, often, a Fermi surface with nonclassical exponents. He argues that the Luttinger liquid is a fixed point, of the same renormalization group that "usually" yields the Landau-Fermi liquid as a unique fixed point. This Luttinger-liquid state, according to Haldane (1981), already embraces a large class of interacting one-dimensional systems and, Anderson has argued, should also include some two-dimensional systems in which the band spectrum is bounded above, i.e., systems with Mott-Hubbard gaps and an upper Hubbard band. Anderson makes this approach the basis for a theory that appears to be useful in calculating normal-state, and some superconducting, properties of high-T_c superconductors.

The fact that charge and spin acquire distinct spectra in the Haldane-Anderson approach, plus the excitement surrounding the possible role of particles with fractional statistics in two dimensions, the anyons of Wilczek, following the demonstration by Kalmeyer and Laughlin (1987) that a gas of anyons has a superconducting ground state, mean (see also Halperin *et al.*, 1989) that many-electron theorists have truly major challenges ahead. Since the early books by Thouless (1961) and by March *et al.* (1967) on many-body theory, the area of application of many-electron techniques has expanded hugely. The correlation problem was important in the early days (see Wigner, 1934, 1938), but now it has moved to the center of the stage. Whether present models are rich enough to embrace much chemistry underlying the attractive interactions between holes in the ceramic oxide superconductors [see, however, the work of Callaway *et al.* (1990) on small cluster calculations using the Hubbard model], the framework existing now for many-body studies surveyed in the present article should be flexible enough to increasingly embrace realistic systems and, in the high-T_c materials, to eventually incorporate band-structure effects in the specific ceramic oxides, as well as the long-range Coulomb repulsion between holes, which seems to be missing from current studies of the Cooper pair binding.

APPENDIX A: MODEL OF TWO-ELECTRON HOMOPOLAR MOLECULE

Here we shall summarize the results of the model of Falicov and Harris (1969) of a two-electron homopolar molecule.

To define their one-band Hamiltonian, it is convenient to use second quantization operators and to restrict the model to four orbitals, one of each spin in each of the two centers. The Hamiltonian then takes the form

$$H = H_\alpha + H_\beta + H_u + H_K \tag{A1}$$

where

$$H_\alpha = \alpha(n_{1\uparrow} + n_{1\downarrow} + n_{2\uparrow} + n_{2\downarrow}) , \tag{A2}$$

$$H_\beta = \beta(c^\dagger_{1\uparrow}c^\dagger_{2\uparrow} + c^\dagger_{1\downarrow}c_{2\downarrow} + c^\dagger_{2\uparrow}c_{1\uparrow} + c^\dagger_{2\downarrow}c_{1\downarrow}) , \tag{A3}$$

$$H_u = U(n_{1\uparrow}n_{1\downarrow} + n_{2\uparrow}n_{2\downarrow}) , \tag{A4}$$

$$H_K = K(n_{1\uparrow}n_{2\downarrow} + n_{1\uparrow}n_{2\downarrow} + n_{1\downarrow}n_{2\uparrow} + n_{1\downarrow}n_{2\downarrow}) . \tag{A5}$$

Here $c^\dagger_{i\sigma}$, $c_{i\sigma}$, and $n_{i\sigma} = c^\dagger_{i\sigma}c_{i\sigma}$ are, respectively, creation, annihilation, and number operators for the orbital of spin centered on nucleus i. H_α and H_β are, respectively, the single-particle diagonal and off-diagonal terms; H_u is the intra-atomic Coulomb repulsion, while H_k is the corresponding interatomic term. The parameters β, U, and K are positive-definite quantities, such that $U > K$.

Since one is considering only two-electron states, the following results can be exploited:

(a) The electron-number operator

$$N = \sum_{i\sigma} n_i\sigma \tag{A6}$$

is completely diagonal and can be replaced everywhere by the number 2; e.g.,

$$H_\alpha = 2\alpha . \tag{A7}$$

(b) The operator

$$N^2 = \sum_{ij\sigma\sigma'} n_{i\sigma}n_{j\sigma'} \tag{A8}$$

is also completely diagonal and can be replaced everywhere by the number 4.

(c) Recalling that

$$n_{i\sigma}n_{i\sigma} \equiv n_{i\sigma} \tag{A9}$$

for any i and σ, we can utilize (a) and (b) immediately above to write the identity

$$4 = 2 + 2(n_{1\uparrow}n_{1\downarrow} + n_{2\uparrow}n_{2\downarrow}) + 2(n_{1\uparrow}n_{2\uparrow} + n_{1\uparrow}n_{2\downarrow} + n_{1\downarrow}n_{2\uparrow} + n_{1\downarrow}n_{2\downarrow}) . \tag{A10}$$

(d) The Hamiltonian can be rewritten

$$H = 2\alpha + K + \mathcal{H} \tag{A11}$$

with

$$\mathcal{H} = H_\beta + H_u + (H_k - K) , \tag{A12}$$

where the final term can be written

$$H_K - K = -K(n_{1\uparrow}n_{1\downarrow} + n_{2\uparrow}n_{2\downarrow}) = -(K/U)H_u . \tag{A13}$$

From the above expressions, or alternatively from simple physical arguments, it can be readily seen that the eigenvalues of H can depend on U and K only through the difference $U - K$. This permits one to write the ground-state energy E as

TABLE V. Matrix elements of H.

	$\|1\uparrow 2\uparrow\rangle$	$\|1\downarrow 2\downarrow\rangle$	$\|1\uparrow 1\downarrow\rangle$	$\|2\uparrow 2\downarrow\rangle$	$\|1\uparrow 2\downarrow\rangle$	$\|2\uparrow 1\downarrow\rangle$
$\langle 1\uparrow 2\uparrow\|$	0	0	0	0	0	0
$\langle 1\downarrow 2\downarrow\|$	0	0	0	0	0	0
$\langle 1\uparrow 1\downarrow\|$	0	0	$U-K$	0	$-\beta$	$-\beta$
$\langle 2\uparrow 2\downarrow\|$	0	0	0	$U-K$	$-\beta$	$-\beta$
$\langle 1\uparrow 2\downarrow\|$	0	0	$-\beta$	$-\beta$	0	0
$\langle 2\uparrow 1\downarrow\|$	0	0	$-\beta$	$-\beta$	0	0

$$E=\langle H\rangle=2\alpha+K+\epsilon\ , \tag{A14}$$

where

$$\epsilon=\langle \mathcal{H}\rangle=\beta\epsilon(x) \tag{A15}$$

with ϵ only dependent on the variable $x=(U/K)/\beta$.

We now discuss the exact ground state.

Any eigenstate of Eq. (A12) with two electrons should be a linear combination of the six states

$$|1\uparrow 2\uparrow\rangle,\ |1\downarrow 2\downarrow\rangle,\ |1\uparrow 1\downarrow\rangle\ ,$$

$$|2\uparrow 2\downarrow\rangle,\ |1\uparrow 2\downarrow\rangle,\ |2\uparrow 1\downarrow\rangle,$$

where

$$|i\sigma j\sigma'\rangle=c_{i\sigma}^{+}c_{j\sigma'}^{+}|0\rangle \tag{A16}$$

with $|0\rangle$ as the vacuum state. The matrix elements of H in this manifold are given in Table V, taken from Falicov and Harris (1969).

An exact diagonalization of the Hamiltonian matrix yields from the ground state $|G\rangle$

$$\begin{aligned}|G\rangle=&2[16+x^2(x^2+16)^{1/2}]^{-1/2}(|1\uparrow 1\downarrow\rangle+|2\uparrow 2\downarrow\rangle)\\&+0.5[x+(x^2+16)^{1/2}]\\&\times[16+x^2+x(x^2+16)^{1/2}]^{-1/2}\\&\times(|1\uparrow 2\downarrow\rangle+|2\uparrow 1\downarrow\rangle)\ ,\end{aligned} \tag{A17}$$

while the energy, expressed in the variables discussed above, is characterized by

$$\epsilon_G=0.5[x-(x^2+16)^{1/2}]\ . \tag{A18}$$

Falicov and Harris have used these exact results to assess the accuracy of various approximate solutions such as the Heitler-London and molecular-orbital solutions discussed in Sec. III.A, but we shall not go into detail here, except to say that the most successful approximate solutions of their model are of the form of symmetrized spin-density-wave trial functions.

The generalization of this model to more complicated, many-electron chains has also been discussed (Fenton, 1968; Harris and Falicov, 1969), and we refer the interested reader to these papers for details.

APPENDIX B: POSITIVITY OF THE STATIC GREEN'S FUNCTION $G(\mathbf{R},\mathbf{R}')$

Here we shall prove that the Green's function $G(\mathbf{R},\mathbf{R}')$, obtained as a solution of Eq. (4.11) with homogeneous boundary conditions, is non-negative. We start by remarking that, with a suitable choice of the constant V_0, all the eigenvalues of the Schrödinger operator $H+V_0$ with homogeneous boundary conditions are positive and in particular the lowest one, $\varepsilon_0\equiv E_0+V_0>0$. Of course the ground-state wave function $\phi_0(\mathbf{R})$ has the same sign everywhere.

From Eq. (4.15), it is evident that $G(\mathbf{R},\mathbf{R}')$ is positive and vanishes only at points $\mathbf{R}'$ where all wave functions are vanishing. Therefore, $G(\mathbf{R}',\mathbf{R}')=0$ also implies $G(\mathbf{R},\mathbf{R}')=0$ for all values of $\mathbf{R}$.

On the other hand, $G(\mathbf{R}',\mathbf{R}')>0$ implies that, for given $\mathbf{R}'$, the function $\tilde{\phi}_0(\mathbf{R})$ defined by

$$\tilde{\phi}_0(\mathbf{R})\equiv G(\mathbf{R},\mathbf{R}'),\quad \text{fixed } \mathbf{R}'\ , \tag{B1}$$

is positive in a region around $\mathbf{R}'$ for reasons of continuity. Let us assume *per absurdum* that regions exist where $\tilde{\phi}_0(\mathbf{R})$ is negative. Let D_2 be the domain where $\tilde{\phi}_0(\mathbf{R})<0$, the point $\mathbf{R}'$ being in its complement D_1, and $D=D_1+D_2$ being the $3N$-dimensional domain of interest. Clearly, nodal surfaces must exist that separate negative and positive regions. It is not difficult to convince oneself that it is always possible to find a subdomain of D_2 (denoted by D'), possibly coinciding with D_2, such that $\tilde{\phi}_0(\mathbf{R})$ does not change sign in D' and vanishes on its boundary. It follows that in the closed domain D' the function $\tilde{\phi}_0(\mathbf{R})$ satisfies

$$(H+V_0)\tilde{\phi}_0(\mathbf{R})=0\ , \tag{B2}$$

with homogeneous boundary conditions. In other words, the Schrödinger operator $H+V_0$, restricted to D' and with the condition that the eigenfunctions vanish at the boundary, possesses the ground-state eigenfunction $\tilde{\phi}_0$ with eigenvalue $\tilde{\varepsilon}_0=0$. Clearly, one has $\varepsilon_0>\tilde{\varepsilon}_0$. However, it can be shown using the calculus of variations (see, for instance, Courant and Hilbert, 1953, particularly Chap. VI,2, theorem 3) that under the present circumstances, i.e., D' is a proper subdomain of D, it must instead hold the condition $\tilde{\varepsilon}_0>\varepsilon_0$. Thus one is led to a contradiction. Therefore $G(\mathbf{R},\mathbf{R}')$ is non-negative.

REFERENCES

Alder, B. J., D. M. Ceperley, and P. J. Reynolds, 1982, J. Chem. Phys. **86**, 1200.

Anderson, J. B., 1975, J. Chem. Phys. **63**, 1499.

Anderson, J. B., 1976, J. Chem. Phys. **65**, 4121.
Anderson, J. B., 1980, J. Chem. Phys. **73**, 3897.
Anderson, P. W., 1973, Mater. Res. Bull. **8**, 153.
Anderson, P. W., 1987, Science **235**, 1196.
Anderson, P. W., 1990, Phys. Rev. Lett. **64**, 1839.
Bachelet, G. B., D. M. Ceperley, and M. G. B. Chiocchetti, 1989, Phys. Rev. Lett. **62**, 2088.
Bamzai, A. S., and B. M. Deb, 1981, Rev. Mod. Phys. **53**, 95.
Barnes, S. E., 1976, J. Phys. F **6**, 1375.
Baskaran, G., Z. Zou, and P. W. Anderson, 1987, Solid State Commun. **63**, 973.
Baus, M., 1990, J. Phys. Condens. Matter **2**, 2111.
Becke, A. D., 1992, J. Chem. Phys. **96**, 2155.
Bednorz, J. G., and K. A. Müller, 1986, Z. Phys. B **64**, 189.
Benfatto, G., and G. Gallavotti, 1990, Phys. Rev. B **42**, 9967.
Bethe, H. A., 1931, Z. Phys. **71**, 205.
Betsuyaku, M., and I. Yokota, 1986, Phys. Rev. B **33**, 6505.
Blankenbecler, R., D. J. Scalapino, and R. L. Sugar, 1981, Phys. Rev. D **24**, 2278.
Bloch, F., 1928, Z. Phys. **57**, 545.
Bonner, J. C., and M. E. Fisher, 1964, Phys. Rev. **135A**, 640.
Brinkman, W. F., and T. M. Rice, 1970, Phys. Rev. B **2**, 4302.
Callaway, J., and N. H. March, 1984, Solid State Phys. **38**, 136.
Callaway, J., D. P. Chen, D. G. Kanhere, and Qiming-Li, 1990, Phys. Rev. B **42**, 465.
Carr, W. J., 1961, Phys. Rev. **122**, 1437.
Castellani, C., C. Di Castro, D. Feinberg, and J. Ranninger, 1979, Phys. Rev. Lett. **43**, 1957.
Ceperley, D. M., 1978, Phys. Rev. B **18**, 3126.
Ceperley, D. M., 1981, in *Recent Progress in Many-Body Theories,* edited by J. G. Zabolitzky, M. de Llano, M. Fortes, and J. W. Clarck (Springer-Verlag, Berlin), p. 262.
Ceperley, D. M., 1983, J. Comput. Phys. **51**, 404.
Ceperley, D. M., 1986, J. Stat. Phys. **43**, 815.
Ceperley, D. M., and B. J. Alder, 1980, Phys. Rev. Lett. **45**, 566.
Ceperley, D. M., and B. J. Alder, 1984, J. Chem. Phys. **81**, 5833.
Ceperley, D. M., and M. H. Kalos, 1979, in *Monte Carlo Methods in Statistical Physics,* edited by K. Binder (Springer-Verlag, Berlin), p. 145.
Coldwell-Horsfall, R. A., and A. A. Maradudin, 1963, J. Math. Phys. **4**, 582.
Coulson, C. A., and I. Fisher, 1949, Philos. Mag. **40**, 386.
Courant, R., and D. Hilbert, 1953, *Methods of Mathematical Physics, Vol. I* (Interscience, New York), Chap. 6.
Dieterich, K., and P. Fulde, 1987, J. Chem. Phys. **87**, 2976.
Dirac, P. A. M., 1930, Proc. Cambridge Philos. Soc. **26**, 376.
Falicov, L. M., and R. A. Harris, 1969, J. Chem. Phys. **51**, 3153.
Fazekas, P., and P. W. Anderson, 1974, Philos. Mag. **30**, 432.
Fenton, E. W., 1968, Phys. Rev. Lett. **21**, 1427.
Fermi, E., 1928, Z. Phys. **48**, 73.
Ferraz, A., P. J. Grout, and N. H. March, 1978, Phys. Lett. A **66**, 155.
Fiorentini, V., and A. Baldereschi, 1992, J. Phys. Condens. Matter **4**, 5967.
Foldy, L. L., 1971, Phys. Rev. B **3**, 3472.
Gebhard, F., and D. Vollhardt, 1987, Phys. Rev. Lett. **59**, 1472.
Gell-Mann, M., and K. A. Brueckner, 1957, Phys. Rev. **106**, 364.
Ghosh, S. K., and B. M. Deb, 1982, Phys. Rep. **92**, 1.
Godby, R. W., M. Schlüter, and L. J. Sham, 1988, Phys. Rev. B **37**, 10 159.
Gombás, P., 1949, *Die Statistische Theorie des Atoms und ihre Andwendungen* (Springer, Vienna).
Gros, G., R. Joynt, and T. M. Rice, 1987a, Phys. Rev. B **36**, 381.
Gros, G., R. Joynt, and T. M. Rice, 1987b, Z. Phys. B **68**, 425.
Gutzwiller, M. C., 1963, Phys. Rev. Lett. **10**, 159.
Gutzwiller, M. C., 1964, Phys. Rev. **134**, A923.
Gutzwiller, M. C., 1965, Phys. Rev. **137**, A1726.
Haldane, F. D. M., 1981, J. Phys. C **14**, 2585.
Halperin, B. I., J. March-Russell, and F. Wilczek, 1989, Phys. Rev. B **40**, 8726.
Hammond, B. L., P. J. Reynolds, and W. A. Lester, Jr., 1987, J. Chem. Phys. **87**, 1130.
Hammond, B. L., P. J. Reynolds, and W. A. Lester, Jr., 1988, Phys. Rev. Lett. **61**, 2312.
Harris, R. A., and L. M. Falicov, 1969, J. Chem. Phys. **50**, 4590.
Heitler, W., and F. London, 1927, Z. Phys. **44**, 455.
Hirsch, J. E., 1983, Phys. Rev. B **28**, 4059.
Hirsch, J. E., 1985, Phys. Rev. Lett. **54**, 1317.
Hirsch, J. E., 1986, J. Stat. Phys. **43**, 841.
Hirsch, J. E., and S. Tang, 1989, Phys. Rev. Lett. **62**, 591.
Hohenberg, P., and W. Kohn, 1964, Phys. Rev. **136**, B864.
Holas, A., and N. H. March, 1991, Phys. Lett. **157**, 160.
Horsch, P., and P. Fulde, 1979, Z. Phys. B **36**, 23.
Horsch, P., and T. Kaplan, 1983, J. Phys. C **10**, L1203.
Huang, C., J. A. Moriarty, and A. Sher, 1976, Phys. Rev. B **14**, 2539.
Hubbard, J., 1959, Phys. Lett. **3**, 77.
Hunter, G., and N. H. March, 1989, Int. J. Quantum Chem. **35**, 649.
Hurley, M. M., and P. A. Christiansen, 1987, J. Chem. Phys. **86**, 1069.
Ichimaru, S., 1982, Rev. Mod. Phys. **54**, 1017.
Johnson, B. G., P. M. W. Gill, and J. Pople, 1993, J. Chem. Phys. **98**, 5612.
Jones, R. O., and O. Gunnarsson, 1989, Rev. Mod. Phys. **61**, 689.
Kajzar, F., and J. Friedel, 1987, Phys. Rev. B **35**, 9614.
Kalmeyer, V., and R. B. Laughlin, 1987, Phys. Rev. Lett. **59**, 2095.
Kalos, M. H., 1984, in *Monte Carlo Method in Quantum Physics,* NATO ASI Series, edited by M. H. Kalos (Reidel, Dordrecht), p. 19.
Kalos, M. H., D. Levesque, and L. Verlet, 1974, Phys. Rev. A **9**, 2178.
Kaplan, T. A., P. Horsch, and J. Borysowicz, 1987, Phys. Rev. B **35**, 1877.
Kaplan, T. A., P. Horsch, and P. Fulde, 1982, Phys. Rev. Lett. **49**, 889.
Kiel, B., G. Stollhoff, C. Weigel, P. Fulde, and H. Stoll, 1982, Z. Phys. B **46**, 1.
Kohn, W., and L. J. Sham, 1965, Phys. Rev. **140**, A1133.
Koonin, S. E., G. Sugiyama, and H. Friedrich, 1982, in *Time Dependent Hartree-Fock and Beyond,* edited by K. Goeke and P. G. Reinhard (Springer-Verlag, Berlin), p. 214.
Kotliar, G., and A. E. Ruckenstein, 1986, Phys. Rev. Lett. **57**, 1362.
Kotrla, M., 1990, Phys. Lett. A **145**, 33.
Lieb, E. H., and F. Y. Wu, 1968, Phys. Rev. Lett. **20**, 1445.
Lundqvist, S., and N. H. March, 1983, Eds., *Theory of Inhomogeneous Electron Gas* (Plenum, New York).
Luther, A. M., 1979, Phys. Rev. B **19**, 320.
March, N. H., 1957, Adv. Phys. **6**, 1.
March, N. H., 1975, *Self-Consistent Fields in Atoms* (Pergamon, Oxford).
March, N. H., and M. Parrinello, 1982, *Collective Effects in Solids and Liquids* (Hilger, Bristol).

March, N. H., M. Suzuki, and M. Parrinello, 1979, Phys. Rev. B **19**, 2027.
March, N. H., and W. H. Young, 1959, Philos. Mag. **4**, 384.
March, N. H., W. H. Young, and S. Sampanthar, 1967, *The Many-Body Problem in Quantum Mechanics* (Cambridge University, Cambridge, England).
Mårtensson-Pendrill, A., S. A. Alexander, L. Adamowicz, N. Oliphant, J. Olsen, P. Öster, H. M. Quiney, S. Salomonson, and D. Sundholm, 1991, Phys. Rev. A **43**, 3355.
Mattheiss, L. F., 1961, Phys. Rev. **123**, 1209.
Mentch, F., and J. B. Anderson, 1981, J. Chem. Phys. **74**, 6307.
Metzner, W., and D. Vollhardt, 1987, Phys. Rev. Lett. **59**, 121.
Meyer, W., 1971, Int. J. Quantum Chem. Quantum Chem. Symp. No. 5, 341.
Micnas, R., J. Ranninger, and S. Robaszkiewicz, 1990, Rev. Mod. Phys. **62**, 113.
Miglio, L., M. P. Tosi, and N. H. March, 1981, Surf. Sci. **111**, 119.
Moreo, A., D. J. Scalapino, R. L. Sugar, S. R. White, and N. E. Bickers, 1990, Phys. Rev. B **41**, 2313.
Moroni, S., D. M. Ceperley, and G. Senatore, 1992, Phys. Rev. Lett. **69**, 1837.
Moroni, S., and G. Senatore, 1991, Phys. Rev. B **44**, 9864.
Moroni, S., G. Senatore, and D. M. Ceperley, 1993, unpublished.
Moskowitz, J. W., and M. H. Kalos, 1981, Int. J. Quantum Chem. **20**, 1107.
Moskowitz, J. W., and K. E. Schmidt, 1986, J. Chem. Phys. **85**, 2868.
Moskowitz, J. W., K. E. Schmidt, M. A. Lee, and M. H. Kalos, 1982a, J. Chem. Phys. **76**, 1064.
Moskowitz, J. W., K. E. Schmidt, M. A. Lee, and M. H. Kalos, 1982b, J. Chem. Phys. **77**, 349.
Murrell, J. N., 1971, *The Theory of the Electronic Spectra of Organic Molecules* (Chapman and Hall, London).
Negele, J. W., and H. Orland, 1988, *Quantum Many-Particle Systems* (Addison-Wesley, Redwood City, CA), p. 332.
Ogawa, T., K. Kanda, and T. Matsubara, 1975, Prog. Theor. Phys. **53**, 614.
Oles, A. M., F. Pfirsch, and P. Fulde, 1986, J. Chem. Phys. **85**, 5183.
Overhauser, A. W., 1985, Int. J. Quantum Chem. **S14**.
Parr, G., and W. Yang, 1989, *Density Functional Theory of Atoms and Molecules* (Oxford University, Oxford).
Pauling, L., 1949, *The Nature of the Chemical Bond* (Cornell University, Ithaca).
Perdew, J. P., and A. Zunger, 1981, Phys. Rev. B **23**, 5048.
Pickett, W. E., 1986, Comments Solid State Phys. **12**, 1 (Part I) and 57 (Part II).
Reger, J. D., and A. P. Young, 1988, Phys. Rev. B **37**, 5978.
Reynolds, P. J., D. M. Ceperley, B. J. Alder, and W. A. Lester, 1982, J. Chem. Phys. **77**, 5593.
Rosenberg, B. J., and I. Shavitt, 1975, J. Chem. Phys. **63**, 2162.
Scalapino, D. J., and R. L. Sugar, 1981, Phys. Rev. B **24**, 4295.
Schmidt, K. E., and M. H. Kalos, 1984, in *Application of the Monte Carlo Method in Statistical Physics,* edited by K. Binder (Springer-Verlag, Berlin), p. 125.
Senatore, G., and G. Pastore, 1990, Phys. Rev. Lett. **64**, 303.
Sham, L. J., and M. Schlüter, 1983, Phys. Rev. Lett. **51**, 1888.
Shavitt, I., B. Ross, and B. O. Siegbahn, 1977, in *Modern Theoretical Chemistry, Vol. 3,* edited by H. F. Schaefer, III (Plenum, New York), p. 189.
Singwi, K. S., and M. P. Tosi, 1981, Solid State Phys. **36**, 177.
Singwi, K. S., M. P. Tosi, R. H. Land, and A. Sjölander, 1968, Phys. Rev. **176**, 589.
Slater, J. C., 1951, Phys. Rev. **81**, 385.
Sorella, S., 1989, Ph.D. thesis (ISAS, Trieste).
Stollhoff, G., and K. P. Bohnen, 1988, Phys. Rev. B **37**, 4678.
Stollhoff, G., and P. Fulde, 1977, Z. Phys. B **26**, 257.
Stollhoff, G., and P. Fulde, 1978, Z. Phys. B **29**, 231.
Stollhoff, G., and P. Fulde, 1980, J. Chem. Phys. **73**, 4548.
Stratonovich, R. D., 1957, Dokl. Akad. Nauk SSSR **115**, 1097 [Sov. Phys. Dokl. **2**, 416 (1958)].
Sugiyama, G., and S. E. Koonin, 1986, Ann. Phys. (N.Y.) **168**, 1.
Takahashi, M., 1977, J. Phys. C **10**, 1289.
Tan, L., Q. Li, and J. Callaway, 1991, Phys. Rev. B **44**, 341.
Thomas, L. H., 1926, Proc. Cambridge Philos. Soc. **23**, 542.
Thouless, D. J., 1961, *The Quantum Mechanics of Many-Body Systems* (Academic, New York).
Umrigar, C. J., K. J. Runge, and M. P. Nightingale, 1991, in *Monte Carlo Methods in Theoretical Physics,* edited by S. Caracciolo and A. Fabrocini (ETS Editrice, Pisa), p. 161.
van Kampen, N. G., 1981, *Stochastic Processes in Physics and Chemistry* (North-Holland, Amsterdam).
Vollhardt, D., 1984, Rev. Mod. Phys. **56**, 99.
Vosko, S. H., L. Wilk, and M. Nusair, 1980, Can. J. Phys. **58**, 1200.
Wendin, G., 1986, Comments Mod. Phys. D **17**, 115.
White, S. R., D. J. Scalapino, R. L. Sugar, E. Y. Loh, J. E. Gubernatis, and R. T. Scalettar, 1989, Phys. Rev. B **40**, 506.
Wigner, E. P., 1934, Phys. Rev. **46**, 1002.
Wigner, E. P., 1938, Trans. Faraday Soc. **34**, 678.
Wilson, S., 1981, in *Theoretical Chemistry, Vol. 4* (Royal Society of Chemistry, London), p. 1.
Yokoyama, H., and H. Shiba, 1987a, J. Phys. Soc. Jpn. **56**, 1490.
Yokoyama, H., and H. Shiba, 1987b, J. Phys. Soc. Jpn. **56**, 3570.
Yoshida, T., and K. Iguchi, 1988, J. Chem. Phys. **88**, 1032.